

CASE FILE COPY

N 62 65868

MR April 1944

NATIONAL ADVISORY COMMITTEE FOR AERONAUTICS

WARTIME REPORT

ORIGINALLY ISSUED

April 1944 as
Memorandum Report

FLIGHT MEASUREMENTS OF HORIZONTAL TAIL LOADS ON A
TYPICAL PROPELLER-DRIVEN PURSUIT AIRPLANE DURING
STALLED PULL-OUTS AT HIGH SPEED

By Lawrence A. Clousing and William N. Turner

Ames Aeronautical Laboratory
Moffett Field, California



WASHINGTON

NACA WARTIME REPORTS are reprints of papers originally issued to provide rapid distribution of advance research results to an authorized group requiring them for the war effort. They were previously held under a security status but are now unclassified. Some of these reports were not technically edited. All have been reproduced without change in order to expedite general distribution.

NATIONAL ADVISORY COMMITTEE FOR AERONAUTICS

MEMORANDUM REPORT

for the

Materiel Command, U.S. Army Air Forces

FLIGHT MEASUREMENTS OF HORIZONTAL TAIL LOADS ON A

TYPICAL PROPELLER-DRIVEN PURSUIT AIRPLANE

DURING STALLED PULL-OUTS AT HIGH SPEED

By Lawrence A. Clousing and William N. Turner

SUMMARY

Flight measurements were made of the pressures on the horizontal tail surfaces of a typical propeller-driven pursuit airplane during stalled pull-outs at high Mach number. The results indicated that the load distribution during the pull-outs was considerably different from that prescribed by air-load requirements at the time the airplane was designed, and that large tail-load increments were caused by buffeting air flow over the tail as the wing started to stall.

Data are included which were taken in a pull-out made without exceeding the design maneuvering limits of the airplane, but in which, due to compressibility and buffeting effects not considered in design criteria, a relatively severe failure of the horizontal-tail structure occurred.

INTRODUCTION

While it is known that the magnitude and distribution of the air load experienced by an airplane operating at high Mach numbers vary considerably from that predicted by the extrapolation of data obtained at low speeds, a complete understanding of the subject is handicapped by a lack of experimental data. To afford a better understanding of the phenomenon, the Ames Aeronautical Laboratory is conducting an extensive investigation of the magnitude and distribution of the air loads acting on the lifting surfaces of a high-speed fighter-type airplane.

The specific investigation reported herein provides information on the air loads imposed on the horizontal tail surfaces of a typical

propeller-driven pursuit airplane during several dive pull-outs made within the design maneuvering limits of the airplane and in which the airplane was stalled at relatively high Mach numbers, to various degrees of buffeting intensity. This investigation forms a part of the extensive investigation mentioned above.

DESCRIPTION OF THE TEST AIRPLANE

The airplane used in the tests is a single-place, low-wing, cantilever monoplane. It is powered by a 1200-brake horsepower (take-off rating) V-1710-85 liquid-cooled engine. Figure 1 is a photograph of the airplane as instrumented for the flight tests. Figure 2 is a general arrangement drawing of the airplane. General specifications of the airplane are as follows:

Airplane, general

Span 34.0 ft

Length 30.167 ft

Weight

Gross (normal and approximately as flown) 7629 lb

Center-of-gravity position

(For normal gross weight and approximately as flown). 0.285 M.A.C.

Wing

Airfoil section, root NACA 0015

Airfoil section, tip NACA 23009

Area total, including ailerons and section projected through the fuselage 213.22 sq ft

Angle of incidence (relative to the airplane longitudinal axis) 2.0°

Horizontal tail

Span 13.00 ft

Area	40.99 sq ft
Airfoil section	Symmetrical, average thickness about 8 percent
Stabilizer setting (relative to the airplane longitudinal axis).	2.25°
Elevator area (including 4.3 sq ft of modified Handley-Page balance)	16.89 sq ft
Nominal deflection35° up, 15° down
Tab (piano-hinged flap)	
Span	2.25 ft
Area	0.86 sq ft
Nominal deflection	±15°

The horizontal tail is of conventional construction, with metal-covered aluminum-alloy stabilizer and fabric-covered aluminum-alloy elevator. An insert trim tab is fitted at the inboard trailing edge of the left elevator. The horizontal tail surfaces on this airplane had been reinforced for the tests. The principal features of this reinforcing consisted of riveting a 42-13/16- by 0.057-inch 24ST Alclad aluminum-alloy reinforcing plate centrally to the rear face of the stabilizer rear beam (lightening holes same place and size as in rear beam), and of removing and replacing the rivets in the fittings supporting the outer elevator hinge brackets with AN3-6A bolts.

Extra ribs were put in the elevators to permit rigid installation of pressure measuring orifices at the desired stations. These ribs were of 0.032 S0 aluminum, 2 inches wide, with a 1/4-inch flange bent at right angles to each side.

INSTRUMENTATION

Standard NACA instruments were used to record photographically, as a function of time, quantities from which the following variables could be obtained: indicated airspeed; pressure altitude; normal acceleration; engine manifold pressure; engine rpm; approximate angle of attack of the thrust line; landing-gear position; aileron, elevator,

and rudder position; aileron and elevator forces, rolling, yawing, and pitching velocity; and resultant pressure distribution over portions of the left and right horizontal tail surfaces.

Free-air temperature was determined from an indicator connected to a resistance bulb protruding below the right wing panel. The installation was calibrated for error due to the temperature rise caused by compression of the air at the resistance bulb. The temperature readings were taken in slow ascending or descending flight to minimize lag errors of the instrument.

A free-swiveling airspeed head was mounted on the end of a boom extending about 4 feet ahead of the leading edge of the right wing and located at a spanwise station about 7 feet inboard of the wing tip. The airspeed head consisted of two separate static-pressure tubes (for separate connections to the airspeed recorder and altitude recorder) with a single total-pressure tube located between them. The airspeed and altitude recorders were mounted in the right wing at the base of the boom, thus minimizing lag errors due to pressure change in the tubes under conditions of rapidly changing altitude. The recording and service static heads were calibrated for position error by comparing the readings of the respective altimeters with the known pressure altitude, as the airplane was flown at several speeds past a reference height. It was assumed that the total pressure was measured correctly. Indicated airspeed, as used in this report, was computed according to the formula by which standard airspeed meters are graduated. (Gives true airspeed at standard sea-level conditions.) The formula may be written as follows:

$$V_i = 1703 \left[\left(\frac{H - p}{p_0} + 1 \right)^{0.286} - 1 \right]^{\frac{1}{2}}$$

where

V_i correct indicated airspeed, miles per hour

H free-stream total pressure

p free-stream static pressure

p_0 standard atmospheric pressure at sea level

The horizontal tail surfaces of the test airplane were equipped with pressure orifices, on both the top and bottom surfaces, at the stations indicated by figure 3. The top and bottom orifices at each station were interconnected in such a manner that the resultant pressure at the station was recorded rather than individual pressures at the top and bottom orifices. As the tests reported herein were incidental to other tests being conducted concurrently with the airplane, only those orifices at the stations indicated by a cross on figure 3 were connected to the recording manometer during these tests. The recording manometer, a multiple-cell pressure recorder, was mounted in the rear section of the pilot's canopy and was connected to the pressure orifices in the stabilizer and to tubes leading from the elevator by 0.15-inch-inside-diameter aluminum tubing and short lengths of 0.17-inch-inside-diameter rubber tubing. Because of lack of space, 0.09-inch-inside-diameter rubber tubing was used inside the elevator. The pressure lag characteristics of the pressure recording installation were measured in tests on the ground, and the test results indicated that the pressure lag in the system was small.

The angle of attack of the thrust line was measured by a vane mounted on the forward end of a boom which was located at a spanwise station 7 feet inboard from the left wing tip and which extended 4 feet ahead of the wing leading edge. The angle of attack as measured by this vane, and as presented in this report, has not been corrected for position error.

TEST DATA AND ANALYSIS

The data for four power-off dive pull-outs made in the 20,000- to 25,000-foot altitude range are shown in figures 4 to 15. Each pull-out is presented in three basic figures. The first figure for each dive pull-out is a time history of the data measured in the run in which part (a) presents general variables, part (b) presents tail pressures, and part (c) presents photographic prints of some of the records showing the relative amount of airplane and control-surface buffeting during the run. (The sharp lines appearing on some of the prints in the buffeting region were scratched on the film manually in order to allow easier reading of the records.) The second figure for each dive pull-out, which is divided into parts (a), (b), etc., presents several representative plots of the chordwise load distribution on the tail at various times during the maneuver. The section lift coefficients shown on this figure are all based on the total length of the local chord (stabilizer plus elevator). The third figure for each pull-out is a time history of the unit

spanwise loading at the 60-percent-span point, derived from integration of a number of the curves of the type shown in the second figure, many of which are not presented in the report. The figures for each pull-out will be discussed in turn.

In figures 4, 5, and 6 it is seen that the airplane was pulled in until a mild stall occurred at an airplane lift coefficient of 0.68 and a Mach number of 0.68. The maximum acceleration factor reached was 5.3 at an angle of attack of the thrust line (uncorrected) of 8.5° . The maximum elevator angle used was 7° up. Buffeting was present, apparently, as may be seen from figure 4 (b), to a greater extent on the left tail than on the right. Rapid fluctuations of pressure, amounting to changes of 200 to 300 pounds per square foot, occurred at the leading edge of the stabilizer during the stall. (Any inaccuracy due to lag in the pressure lines will tend to make the recorded load changes too low.) During the main part of the pull-out, as may be seen from figure 5, the load was upward on the stabilizer and downward on the elevator. The maximum recorded pressures and unit span loads for the pull-out shown in figures 4, 5, and 6 are listed in the following table:

Tail surface	Maximum recorded pressure (lb/sq ft)	Maximum unit span load (lb/ft)
Right stabilizer	440 up	205 up
Left stabilizer	600 up	345 up
Right elevator	150 down	115 down
Left elevator	180 down	105 down

At other spanwise stations, of course, the pressures and loads would differ somewhat from those given above.

In figures 7, 8, and 9 it is seen that the airplane was pulled in until a moderately violent stall occurred at a Mach number of about 0.72. The lift coefficient could not be determined as the accelerometer did not function on this flight. The maximum angle of attack

reached was 14° . The maximum elevator angle was 10° up. Buffeting was present again to a greater extent on the left tail than on the right tail. Rapid fluctuations of pressure of well over 300 pounds per square foot occurred at the leading edge of the stabilizer during the buffeting. The maximum recorded pressures and unit span loads in this run are listed in the following table:

Tail surface	Maximum recorded pressure (lb/sq ft)	Maximum unit span load (lb/ft)
Right stabilizer	490 up	255 up
Left stabilizer	520 up	275 up
Right elevator	210 down	140 down
Left elevator	230 down	135 down

In figures 10, 11, and 12 it is seen that the airplane was pulled in until a violent stall occurred at a lift coefficient of about 0.90 and a Mach number of 0.61. The maximum acceleration factor reached was about 6.2 at an angle of attack of 17° . The maximum elevator angle used was 6.5° up. Buffeting was present, again to a greater extent on the left tail than on the right tail. Rapid fluctuations of pressure of 200 to 300 pounds per square foot occurred at the leading edge of the stabilizer during the buffeting. The maximum recorded pressures and unit span loads in this run are listed in the following table:

Tail surface	Maximum recorded pressure (lb/sq ft)	Maximum unit span load (lb/ft)
Right stabilizer	510 up	215 up
Left stabilizer	500 up	235 up
Right elevator	100 down	65 down
Left elevator	180 down	90 down

In figures 13, 14, and 15 it is seen that the airplane was pulled in until a very violent stall occurred at a lift coefficient of 1.01 and a Mach number of 0.67. The maximum acceleration factor reached was 7.5 at an angle of attack of 19° . The maximum elevator angle used was 11.5° up. The buffeting was apparently about the same on both sides of the tail in this run. Rapid fluctuations of pressure of 300 to 400 pounds per square foot occurred at the leading edge of the stabilizer during the buffeting. The maximum recorded pressures and unit span loads in this run are listed in the following table:

Tail surface	Maximum recorded pressure (lb/sq ft)	Maximum unit span load (lb/ft)
Right stabilizer	460 up	310 up
Left stabilizer	580 up	445 up
Right elevator	200 down	120 down
Left elevator	230 down	115 down

During this run structural failure of the horizontal tail occurred. Since the airplane was operating within maneuvering limits which were considered safe by design specifications in use at the time the airplane was designed, it is of interest to examine the nature of the tail failure in relation to the loads measured, and in relation to the necessity for revision of air load requirements and the manner of specifying safe maneuverability limits to a pilot.

The principal failures were on the left side of the tail, although failure had also started on the right side. A rear view of the airplane with undamaged tail is shown in figure 16, and views of the principal failures are presented in figures 17 to 23. The left elevator had buckled downward at about the third outboard row of orifices (figs. 17, 18, and 19), cracking the elevator spar (fig. 20). The elevator nose balance had been forced downward severely enough to break the elevator nose rib on each side of the tail just inside the outboard hinge fitting (figs. 21 and 22). The left stabilizer rear beam was cracked at the inboard hinge bracket, and the two top bolts holding the bracket to the stabilizer rear beam had been sheared completely (fig. 23). Other miscellaneous failures of various degrees of severity occurred to both the stabilizer and elevator structure in the immediate vicinity of all the hinge brackets.

It is difficult to ascertain at just what time in the pull-out the structural failure occurred. Its effect was not noticeable until after steady straight flight had been re-established. Then it was noticed that the longitudinal balance and stability characteristics of the airplane had altered. Figure 13 shows that a sudden decrease of elevator control force occurred at 5.3 seconds while the elevator angle and normal acceleration continued to rise; figure 15 shows a numerical decrease in the elevator load curve at this point also. Again, at 6.2 seconds, as the acceleration is decreasing, there is a sudden increase in elevator control force and recorded elevator angle. It appears, however, that the elevator control at 6.2 seconds may have been applied inadvertently as the ailerons were being deflected to counteract the roll-off occurring during the stall. The lack of effect of the elevator control on the value of the acceleration factor of the airplane was probably due to the stalled attitude of the wing. The increase of acceleration factor at 7.0 seconds, as the elevator control force and elevator angle were decreasing, was probably due to the re-establishment of normal flow over the wing, although the possibility that it was caused by the buckling of the elevator should not be completely discounted.

Figure 24 shows the loading conditions for which the horizontal tail surface was designed. Comparison of this figure with the actual flight measurements (figs. 5, 8, 11, and 14) shows that in many instances the unit loads actually measured on the stabilizer in flight were not only considerably in excess of the design unit loads, but that they occurred in a direction opposite to the design loads. At the leading edge of the elevator, the design unit loads were not exceeded in the pull-outs, at least not at the particular spanwise stations at which measurements were made. However, it was the elevator and a fitting supporting the elevator that failed and not the stabilizer.

Inasmuch as the elevator loads at the time of failure did not appear to have been in excess of those for which the surface was designed, the reasons for the failure of the elevator are not entirely clear. Also, higher elevator down loads had been encountered on a previous flight (fig. 9) at least at the spanwise location at which measurements were made.

It is possible that fatigue of the elevator structure may have contributed to the failure of the elevator and stabilizer fitting, inasmuch as many flights had been made during which the airplane had been flown at high accelerations with severe buffeting. It is also possible that the dynamic loads caused by buffeting may have been responsible for the elevator failure. No doubt the buffeting

loads caused much more severe structural strain than the same loads would have caused if applied under static conditions. In the last pull-out, in which the structural failure occurred (figs. 13, 14, and 15), the buffeting was more severe than in any previous maneuver. In this pull-out an attempt had been made to insure absolutely that the maximum acceleration factor possible to attain had been obtained. A strong pull force was exerted on the stick even after heavy buffeting had set in. A slightly greater elevator angle was used than in the previous pull-outs. It should be realized, too, that the loads which were measured during the buffeting condition may actually have been somewhat greater than those recorded, due to lag in the pressure lines.

A minor, but perhaps not negligible, additional load which may have contributed to the failure was that caused by a bar weighing about 2.4 pounds per foot which extended along the leading edge of the elevator between the two hinge brackets. This bar was used as a mass balance for the elevator. The acceleration reached in the last run increased the effective weight of the bar to about 18 pounds per foot. Under the dynamic conditions accompanying heavy buffeting this weight may have added appreciably to the stresses set up in the nose structure.

From the nature of the records it is apparent that buffeting occurred even before the airplane was completely stalled, and that abrupt and large fluctuations in tail load occurred, with the up-load peaks considerably higher than the maximum up-load before the buffeting set in. For example, in figure 6, in which complete stall did not occur, a change in up-load of 42 pounds per foot occurred on the left tail during an increase in acceleration factor of 3.9, and during the time that no buffeting took place. However, during the buffeting immediately following, peak loads greater by 180 pounds per foot were reached, while the acceleration factor increased further only 0.7. This effect is probably due to the abrupt decrease in downwash over the tail as the wing root starts to stall.

It would appear that the results presented herein have indicated the need for designing the tail structure to withstand the dynamic loads which may be imposed. This becomes all the more apparent when the changes in the speed-strength diagram of an airplane with changes in Mach number are considered. The effect of Mach number on the speed-strength diagram for power-off flight, as obtained from the tests reported herein and data from other tests, is shown in figure 25. It is apparent from this diagram that the decrease in CL_{max} with Mach number has made it possible for buffeting from stall to take place at higher indicated airspeeds than would

be expected if the decrease in $C_{l,max}$ with Mach number were neglected. Also, due to Mach number effects, the buffeting probably occurs at a different angle of attack on the tail at high Mach numbers than at low Mach numbers. Due to the higher aerodynamic loads created by buffeting at higher values of dynamic pressure, a critical design condition now exists at the upper left-hand corner of the speed-strength diagram at high Mach numbers that perhaps is not critical in speed-strength diagrams in which the upper left-hand corner is reached at a relatively low value of Mach number. The speed-strength diagram in its simple form, which fails to take into account changes in stall or buffet boundary with Mach number, apparently no longer completely defines to a pilot the safe operating condition for an airplane from the structural standpoint.

CONCLUDING REMARKS

With the test airplane operated within maneuvering limits which were considered safe by design specifications in use at the time the airplane was designed, unit loads were measured on the stabilizer which were not only considerably in excess of the design unit loads, but which occurred in a direction opposite to the design loads.

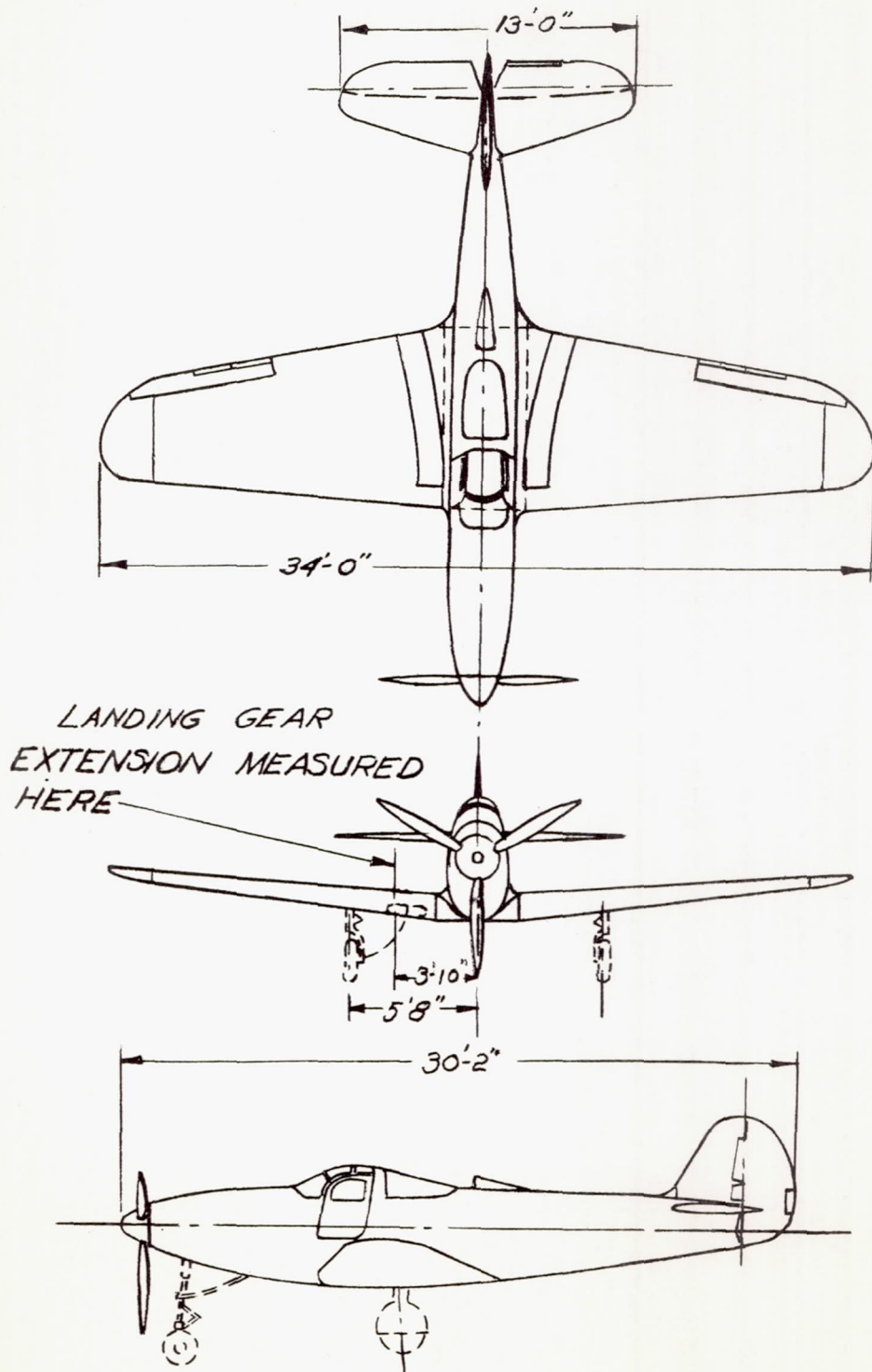
Although there is no evidence that design loads on the elevator were exceeded in the pull-outs, failure of the elevator and a fitting supporting the elevator occurred. It appears from data obtained that the elevator failure was due to a basic cause not considered in design specifications, namely, the reduction of the lift coefficient for stall at high values of Mach number, which allowed the airplane to be subject to severe buffeting without exceeding the design load factor at speeds higher than those computed on the assumption of a constant value of the maximum lift coefficient. The increased energy in the higher speed air stream, coupled with the fluctuating downwash from the stalled wing, may result in loads on the tail surfaces in excess of the design static loads, and in dynamic stresses which may be critical, even though the airplane remains within its design speed and load factor limits.

Revision of the tail-load design requirements and of the manner of specifying safe maneuverability limits to pilots appears necessary.

Ames Aeronautical Laboratory,
National Advisory Committee for Aeronautics,
Moffett Field, Calif.



Figure 1.- Three-quarter rear view of test airplane.



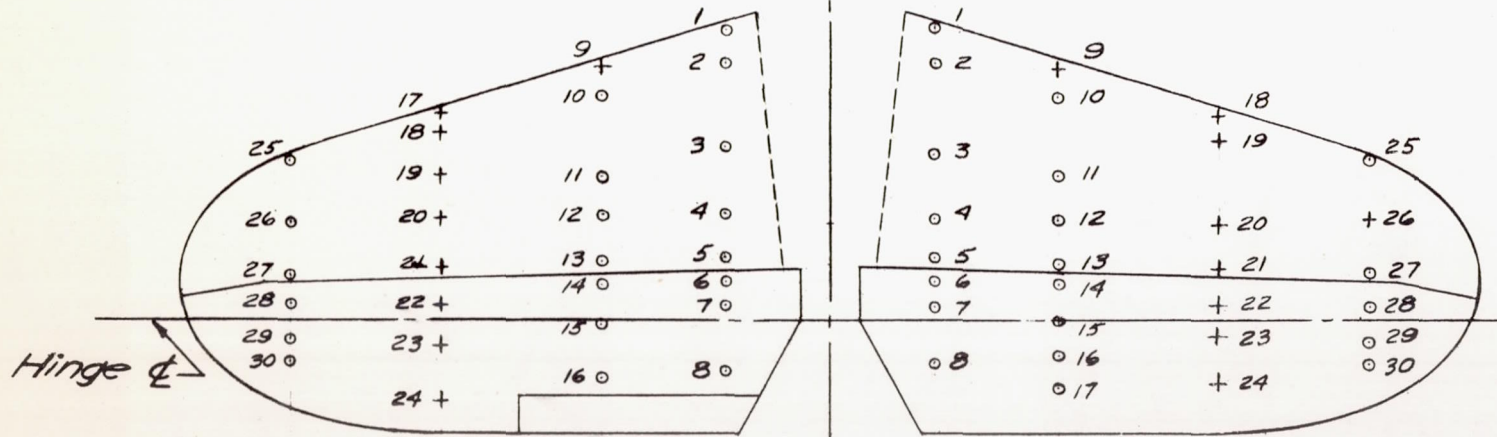
NATIONAL ADVISORY
COMMITTEE FOR AERONAUTICS

FIGURE 2.- THREE-VIEW DRAWING OF THE TEST
AIRPLANE.

Scale : 1 in. = 20 in.

Fuselage ϕ

+ Orifice stations at which pressure was measured.



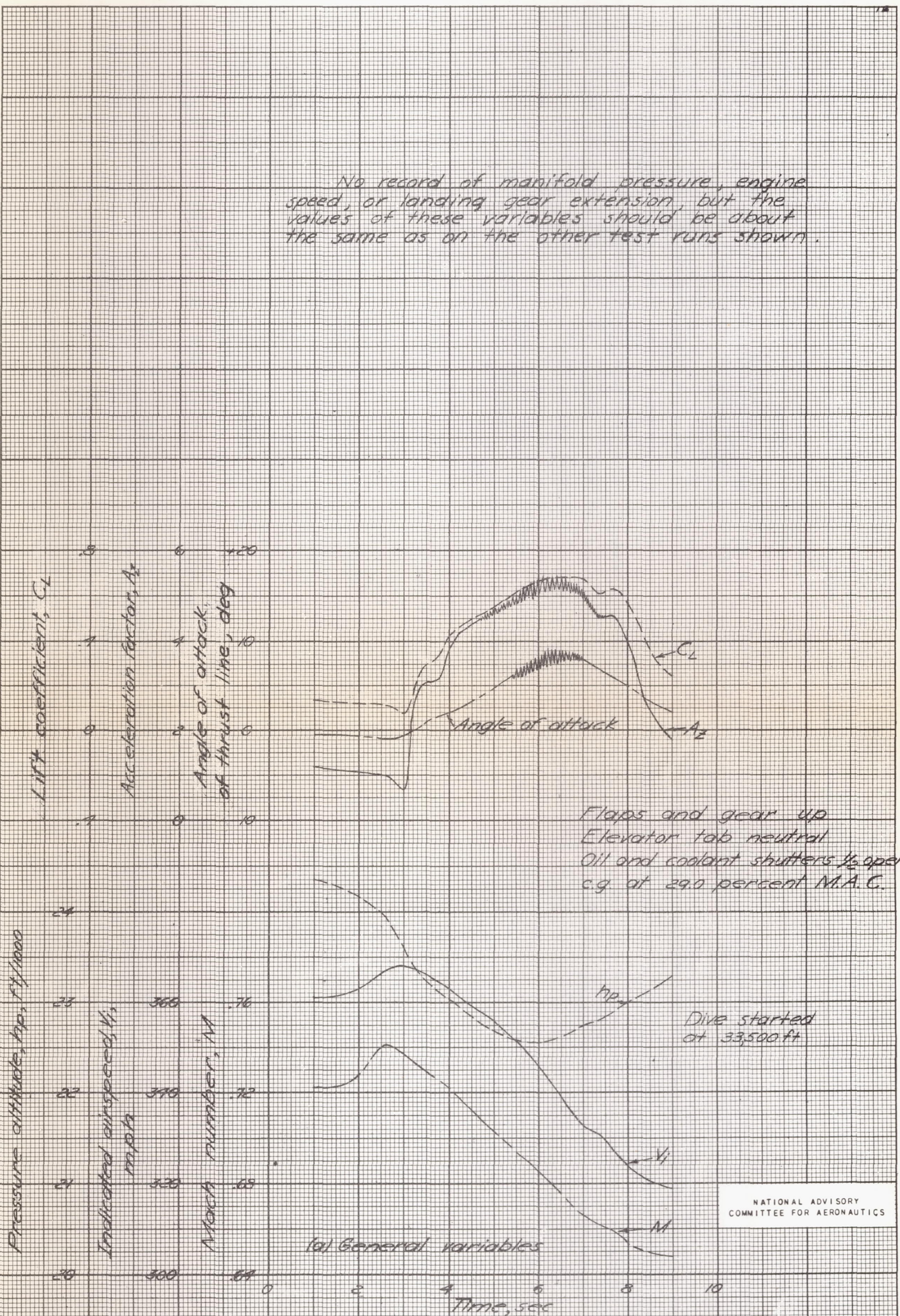
Note: Orifices located on both upper and lower surfaces.

o Orifice stations which were not connected during the subject tests.

NATIONAL ADVISORY
COMMITTEE FOR AERONAUTICS

Figure 3. - Top view of horizontal tail surfaces showing orifice stations at which pressure was measured. Test airplane.

No record of manifold pressure, engine speed, or landing gear extension, but the values of these variables should be about the same as on the other test runs shown.

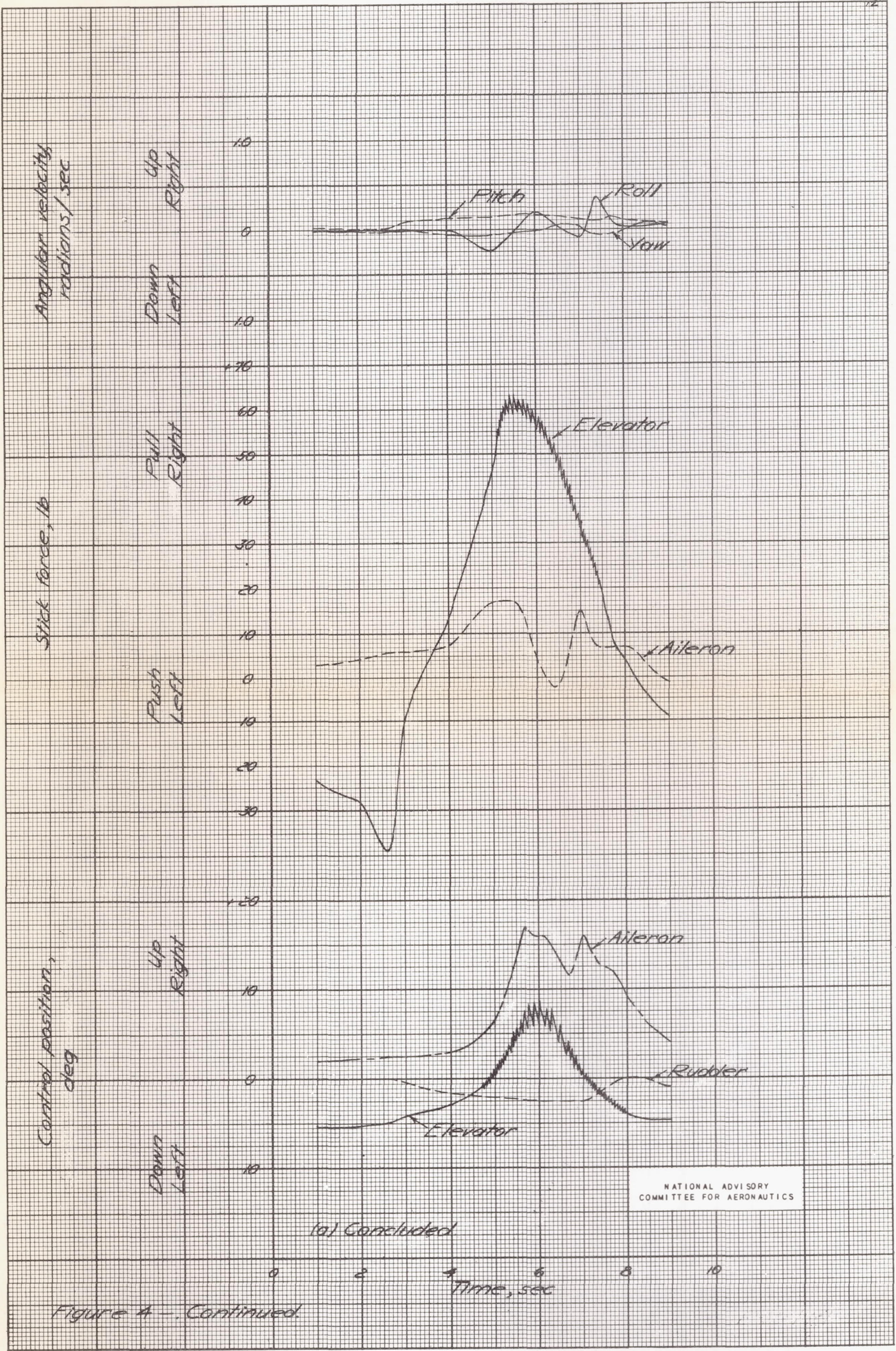


Flaps and gear up
Elevator tab neutral
Oil and coolant shutters $\frac{1}{2}$ open
c.g. at 29.0 percent M.A.C.

Dive started at 33,500 ft

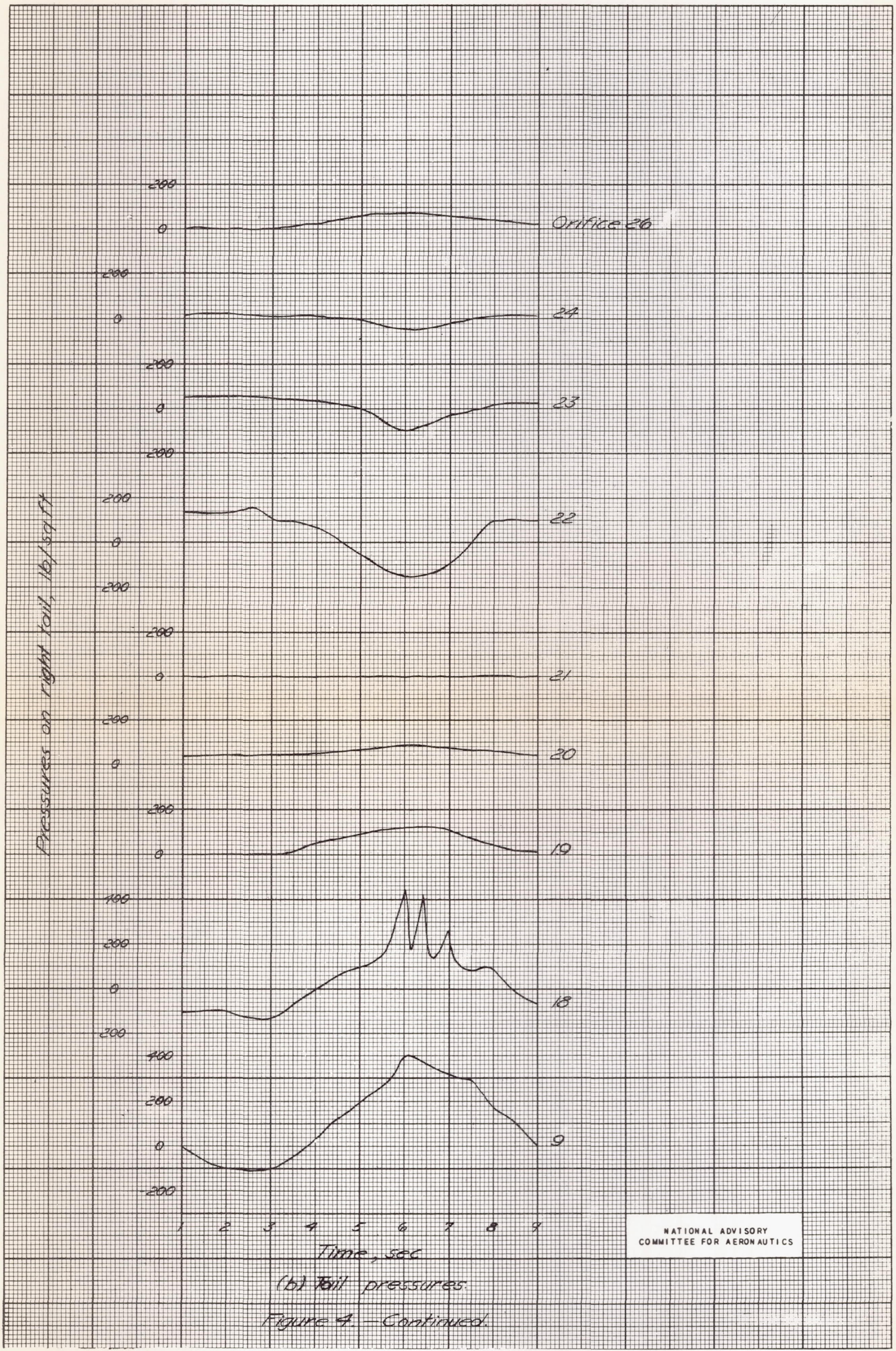
NATIONAL ADVISORY COMMITTEE FOR AERONAUTICS

Figure 4 - Time history of a power-off dive pull-out at $M \approx 0.68$. Test airplane with reinforced stabilizer and elevators.

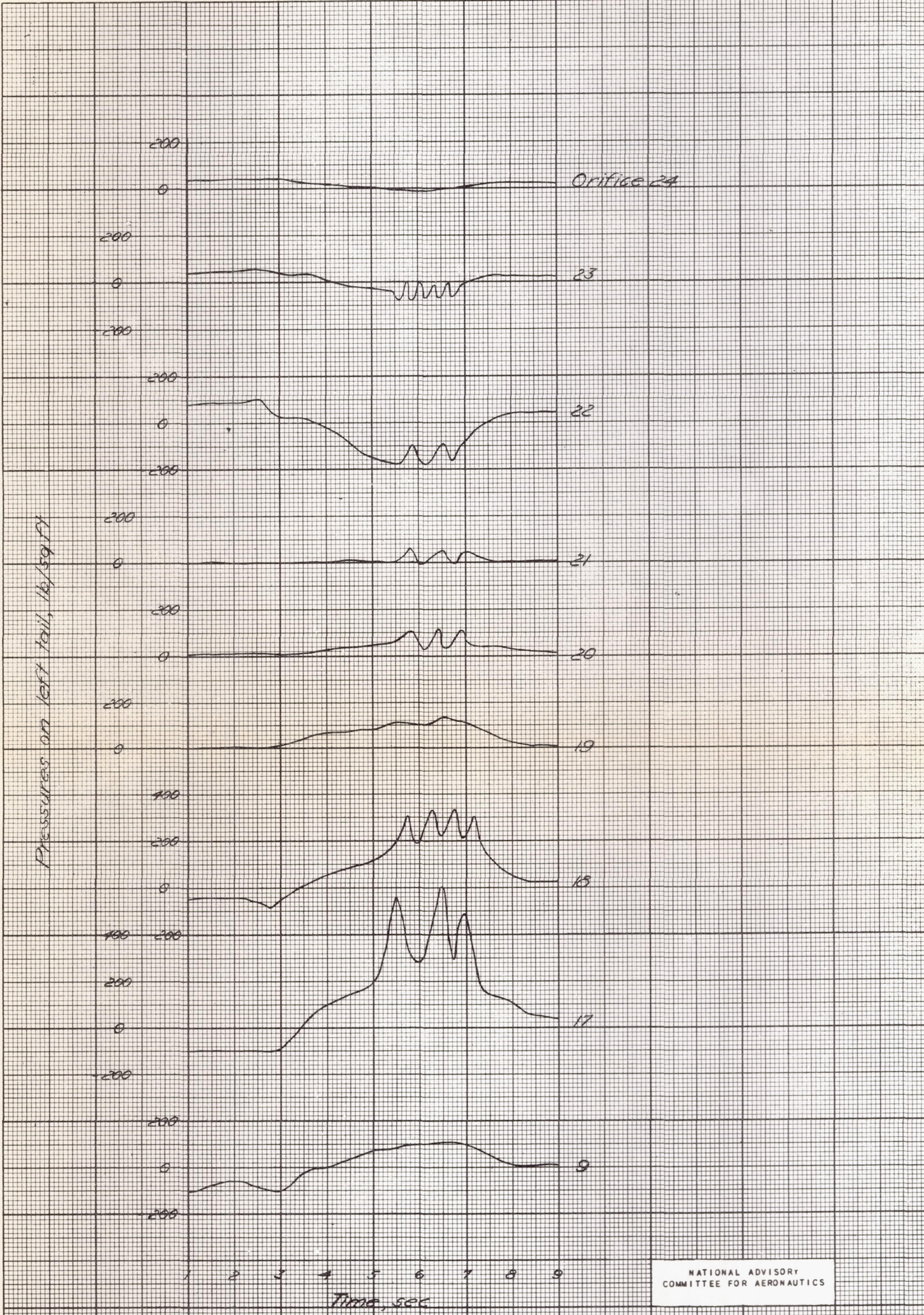


NATIONAL ADVISORY COMMITTEE FOR AERONAUTICS

Figure 4 - Continued.



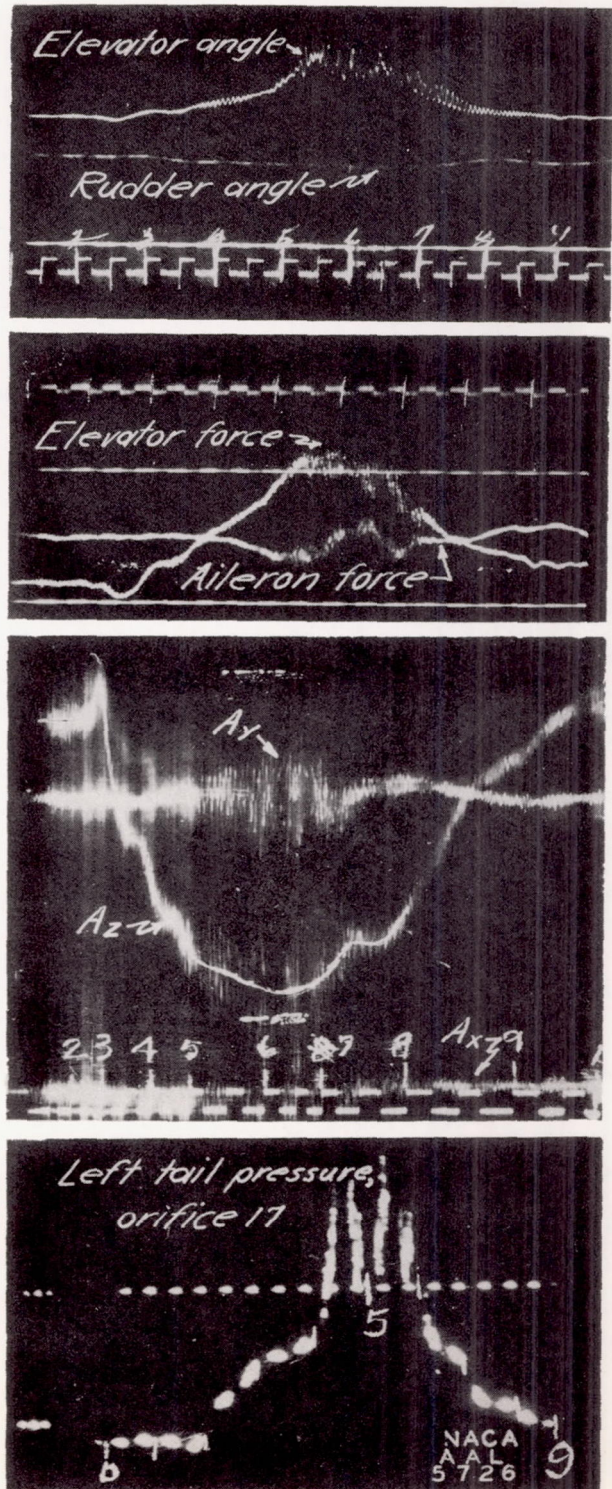
(b) Tail pressures.
Figure 4. - Continued.



NATIONAL ADVISORY
COMMITTEE FOR AERONAUTICS

(b) Concluded.

Figure 4. Continued

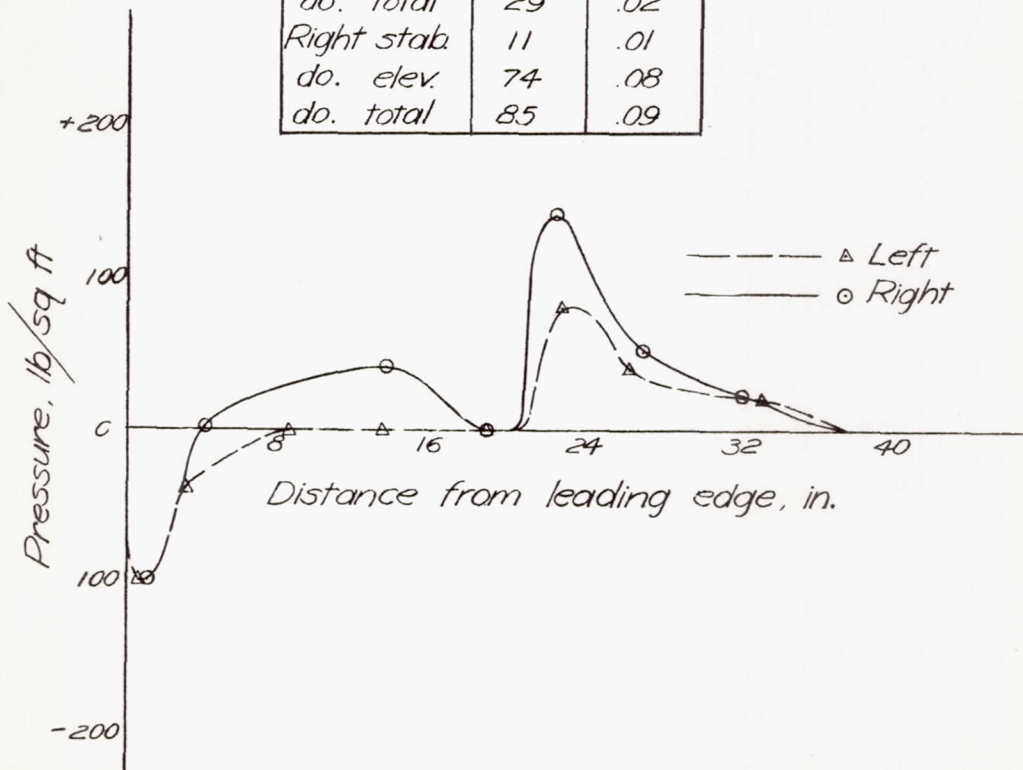


(c) Photographic prints of some of the records showing relative amount of buffeting during the run.

Figure 4.- (Concluded.)

$V_i = 361 \text{ mph}$
 $M = 0.722$
 Altitude 24,350 ft

Chord	lb/ft	C_L
Left stab.	-24	-.03
do. elev.	53	.05
do. total	29	.02
Right stab.	11	.01
do. elev.	74	.08
do. total	85	.09



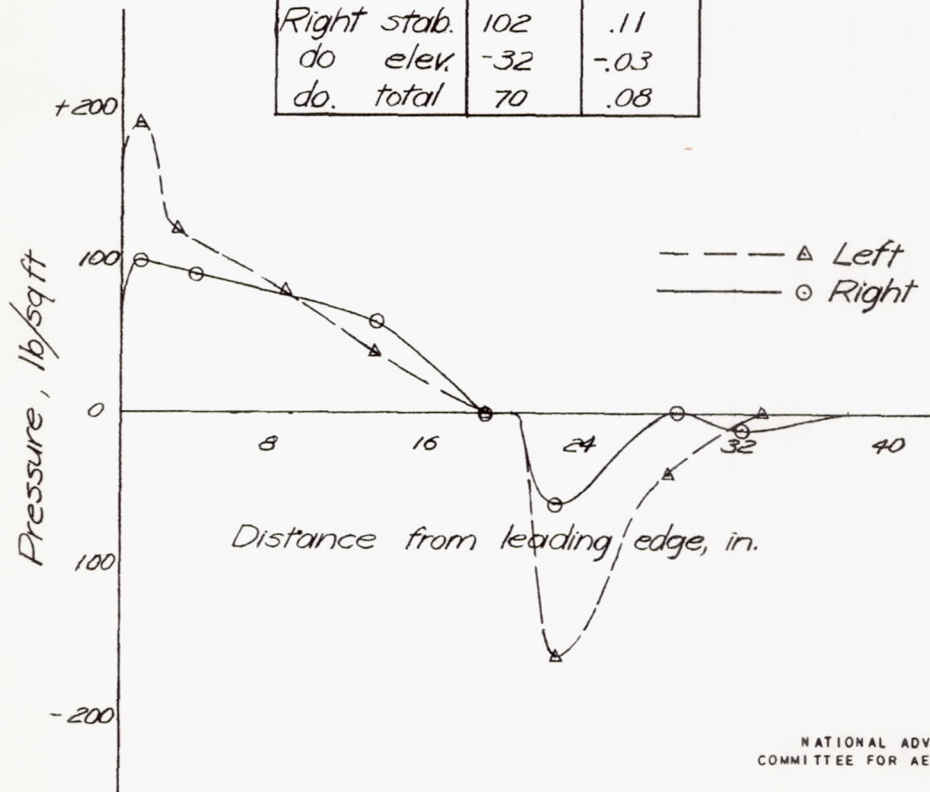
NATIONAL ADVISORY
COMMITTEE FOR AERONAUTICS

(a) At 1.0 second

Figure 5. - Chordwise load distribution at 50 percent semispan in the dive pull-out shown in figure 4.

$V_i = 356 \text{ mph}$
 $M = 0.703$
 Altitude 22,700 ft

Chord	lb/ft	C_L
Left stab.	111	.11
do. elev.	-75	-.08
do. total	36	.03
Right stab.	102	.11
do. elev.	-32	-.03
do. total	70	.08

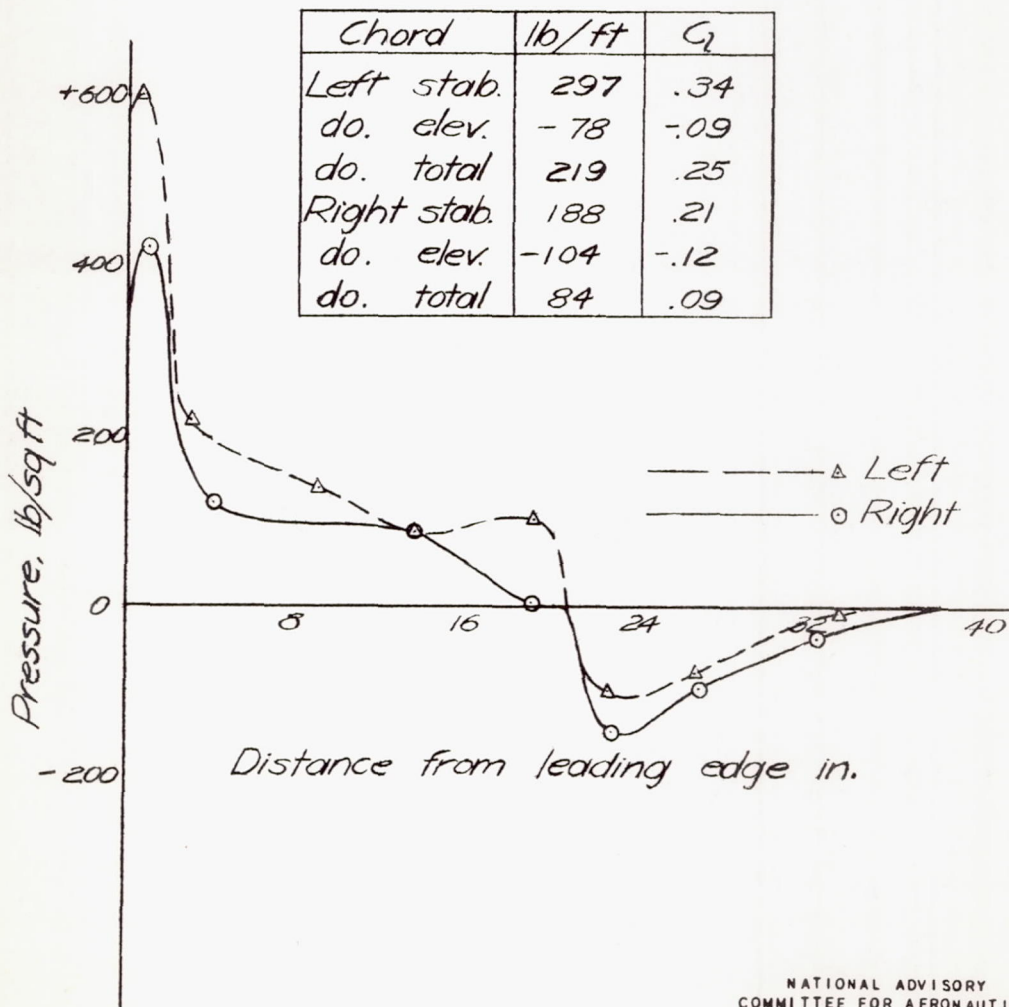


NATIONAL ADVISORY
 COMMITTEE FOR AERONAUTICS

(b) At 50 seconds.

Figure 5.-Continued

$V_i = 340 \text{ mph}$
 $M = 0.674$
 Altitude 22,650ft



NATIONAL ADVISORY
COMMITTEE FOR AERONAUTICS

(c) At 6.5 seconds.

Figure 5.- Concluded

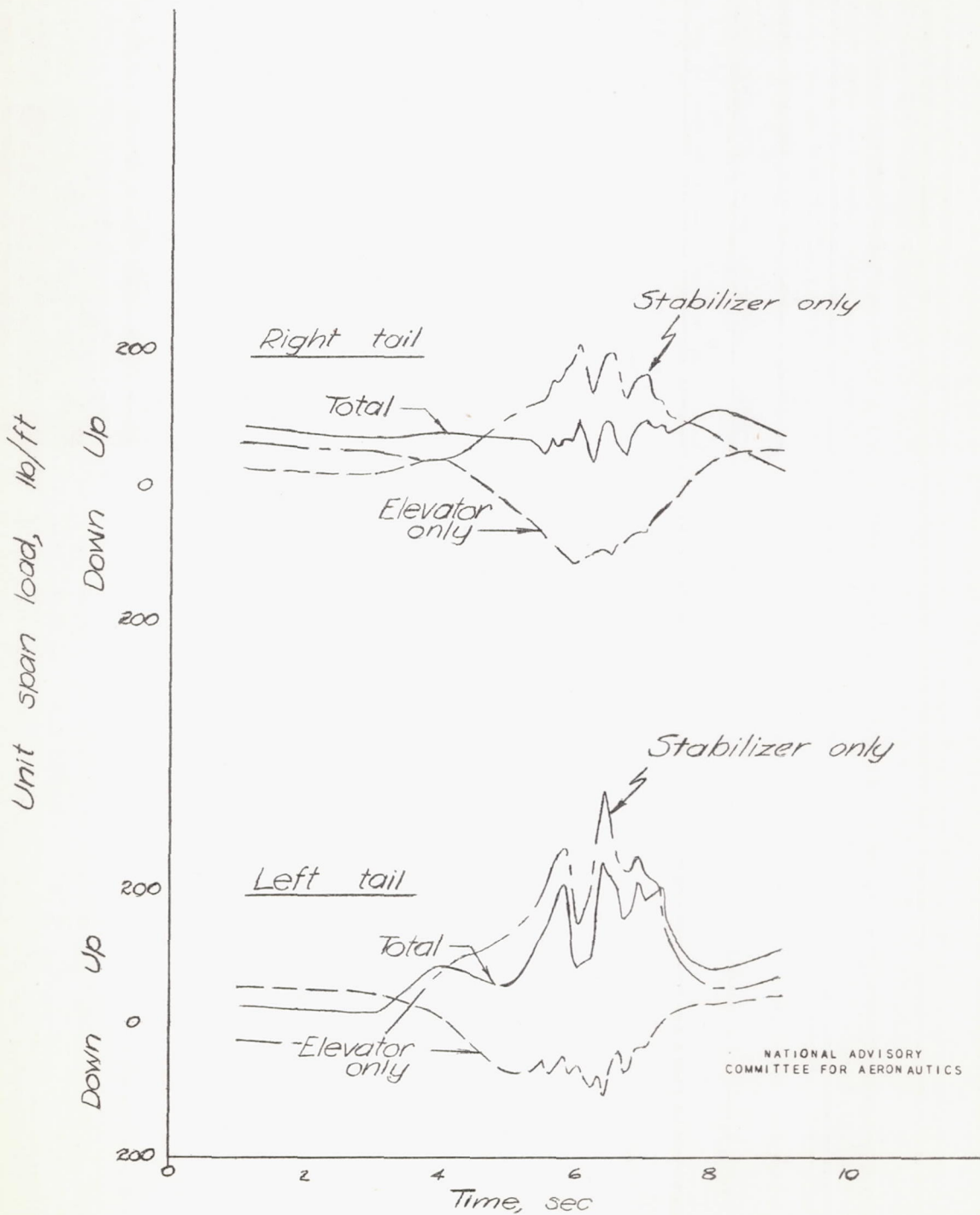


Figure 6.- Time history of the unit span load at 60 percent semispan during the dive pull-out shown in figure 4.

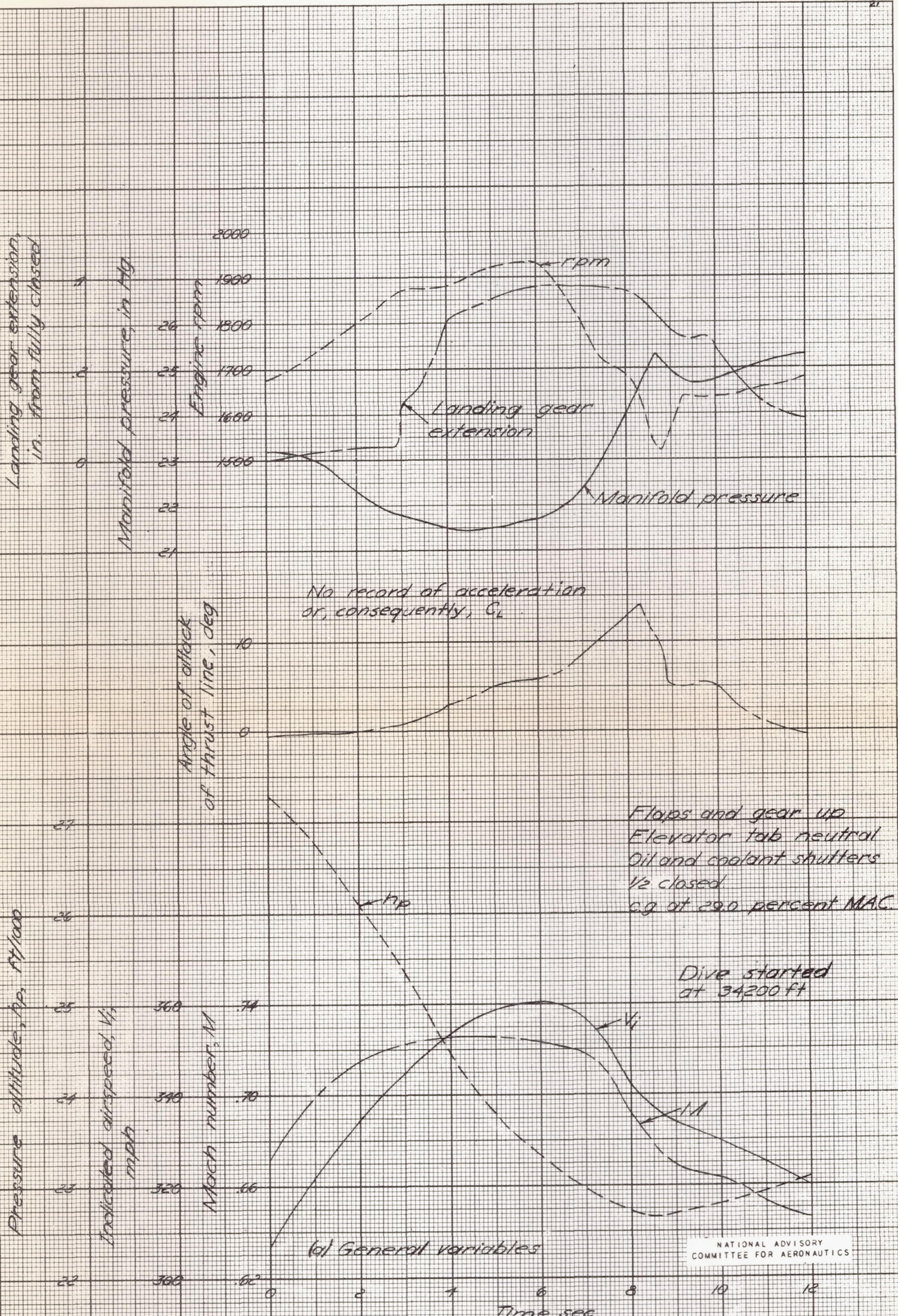


Figure 7 - Time history of a power-off dive pull-out at $M \approx 0.70$.
 Test airplane with reinforced stabilizer and elevators.

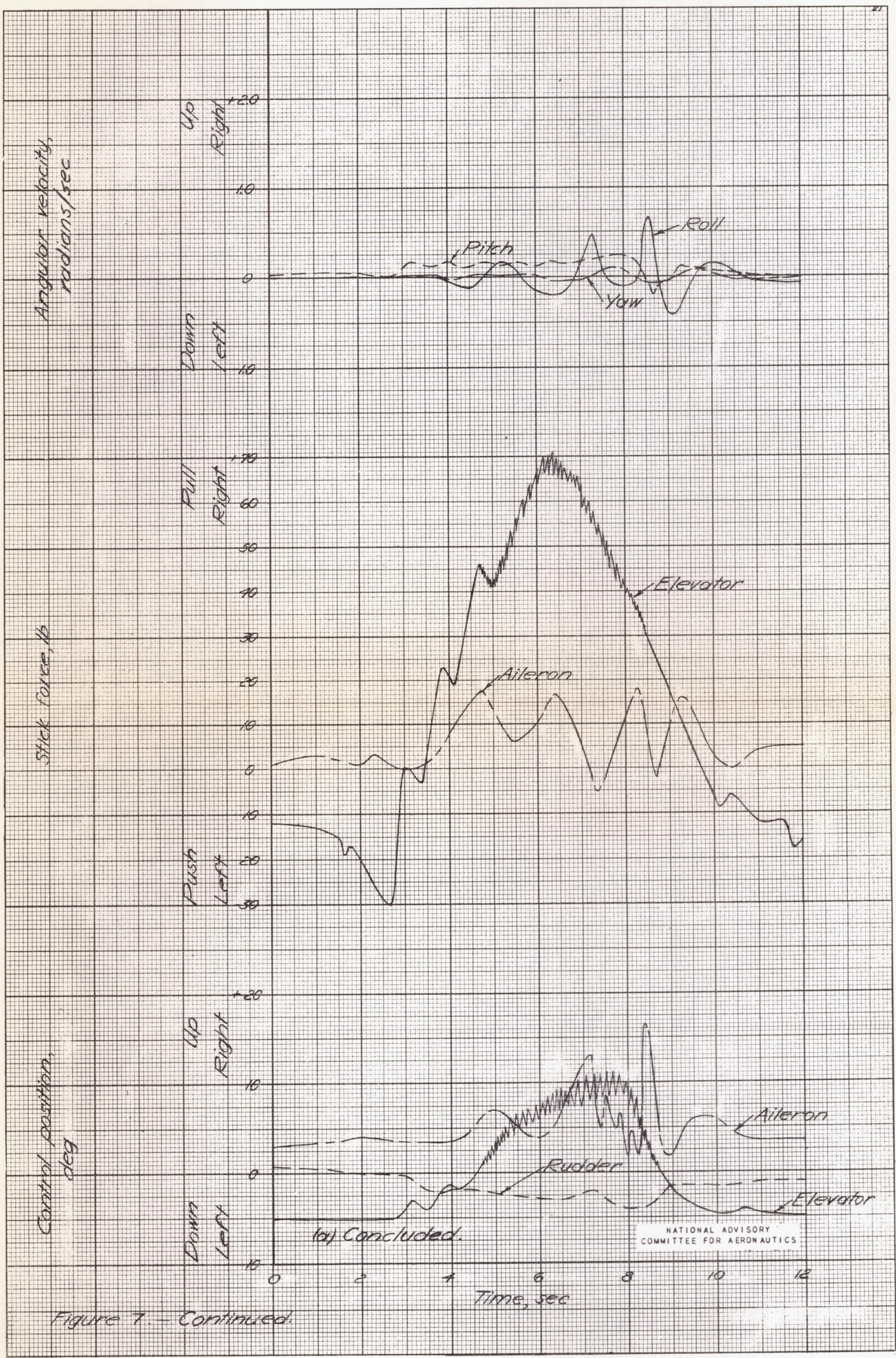
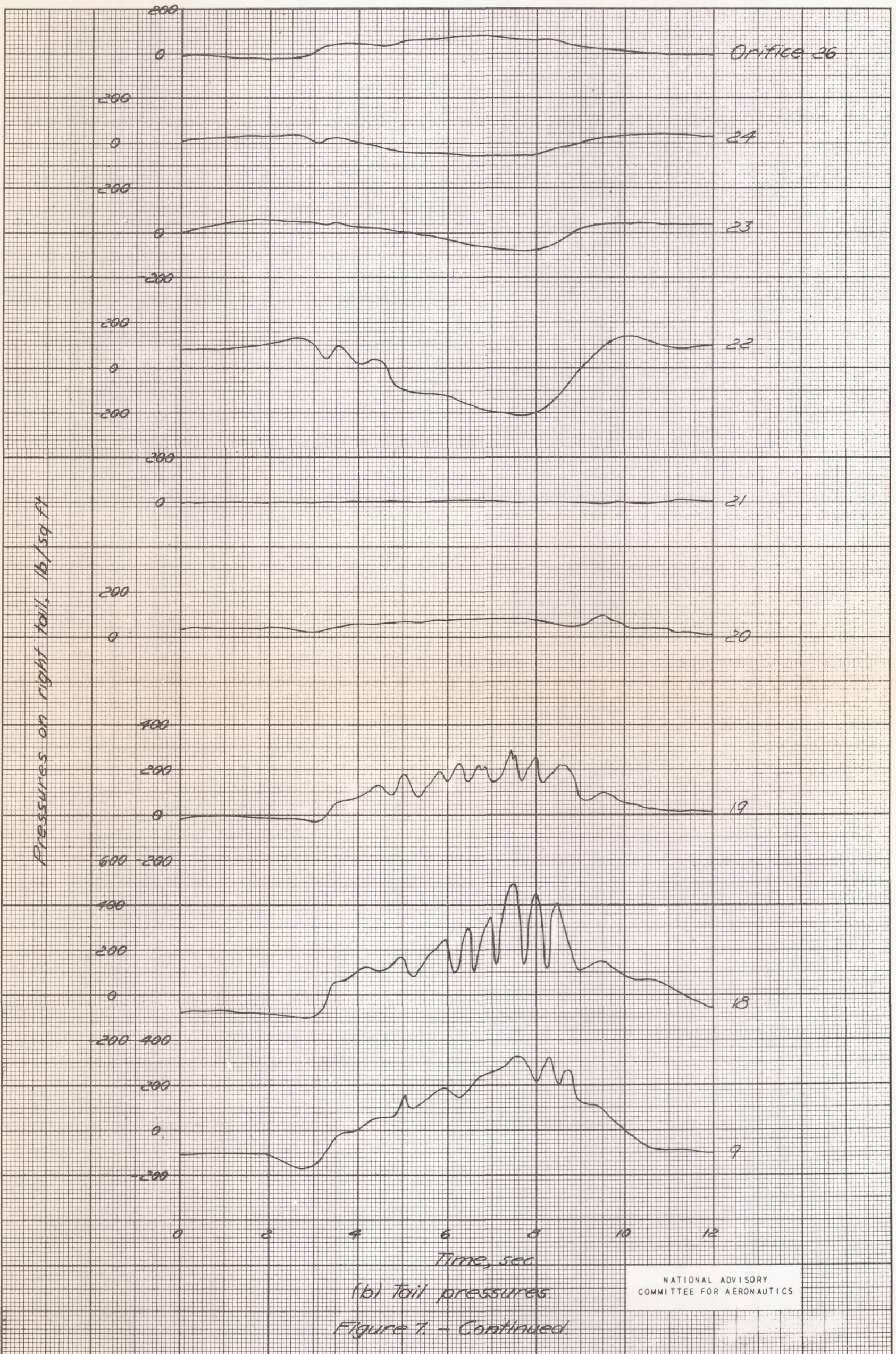
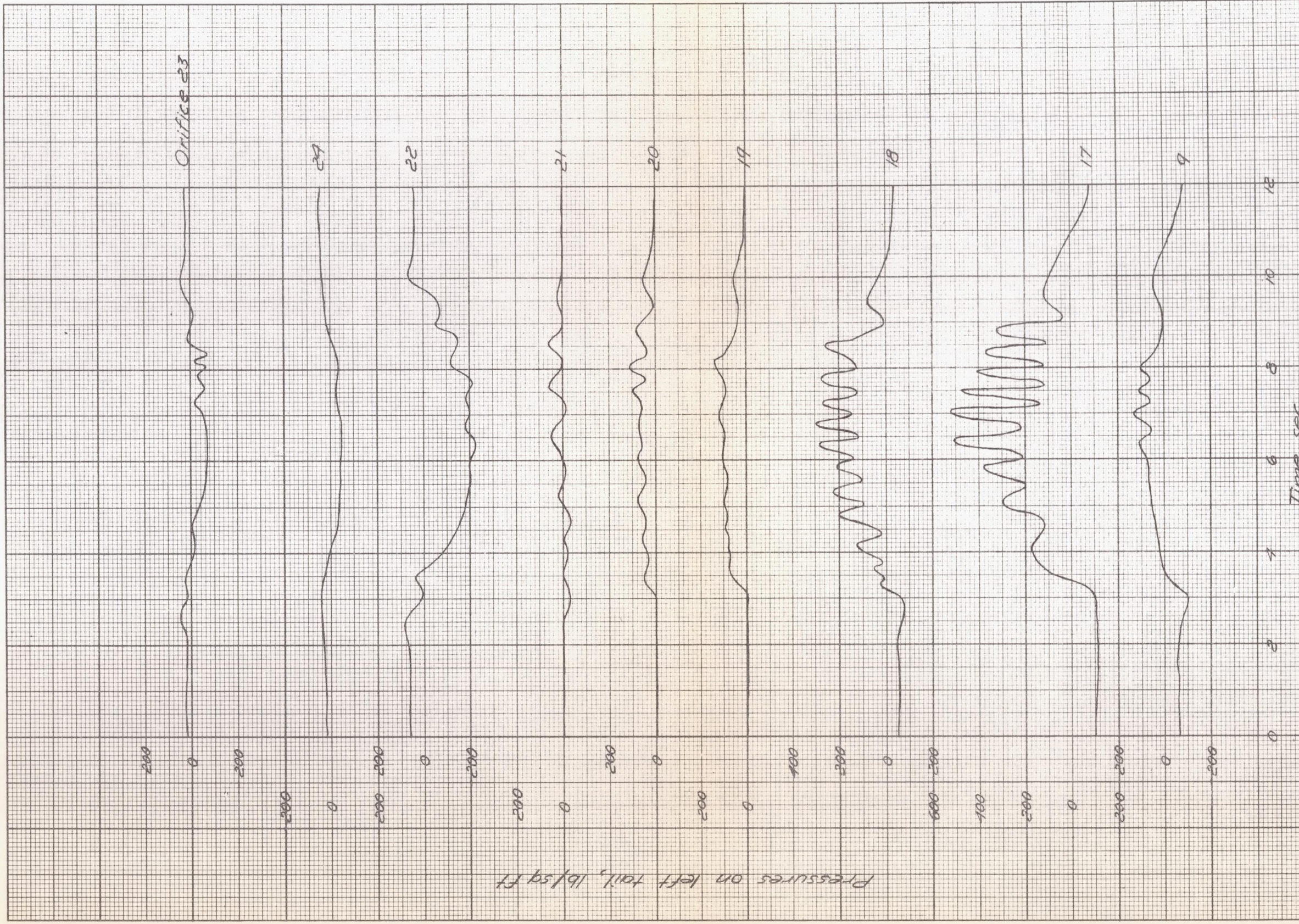


Figure 7. - Continued.

NATIONAL ADVISORY COMMITTEE FOR AERONAUTICS



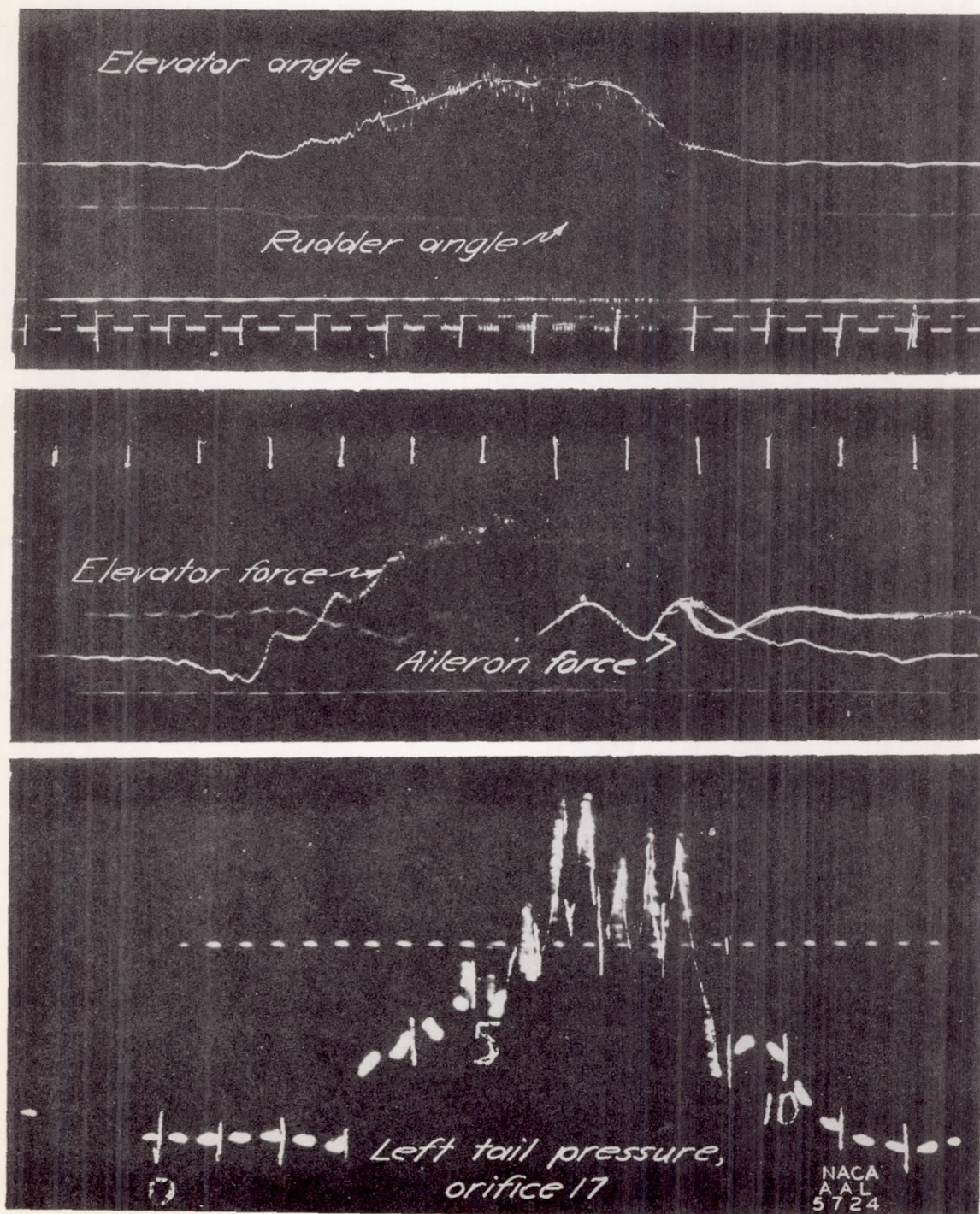
(b) Tail pressures
Figure 7. - Continued.



NATIONAL ADVISORY
COMMITTEE FOR AERONAUTICS

(b) Concluded.

Figure 7 - Continued

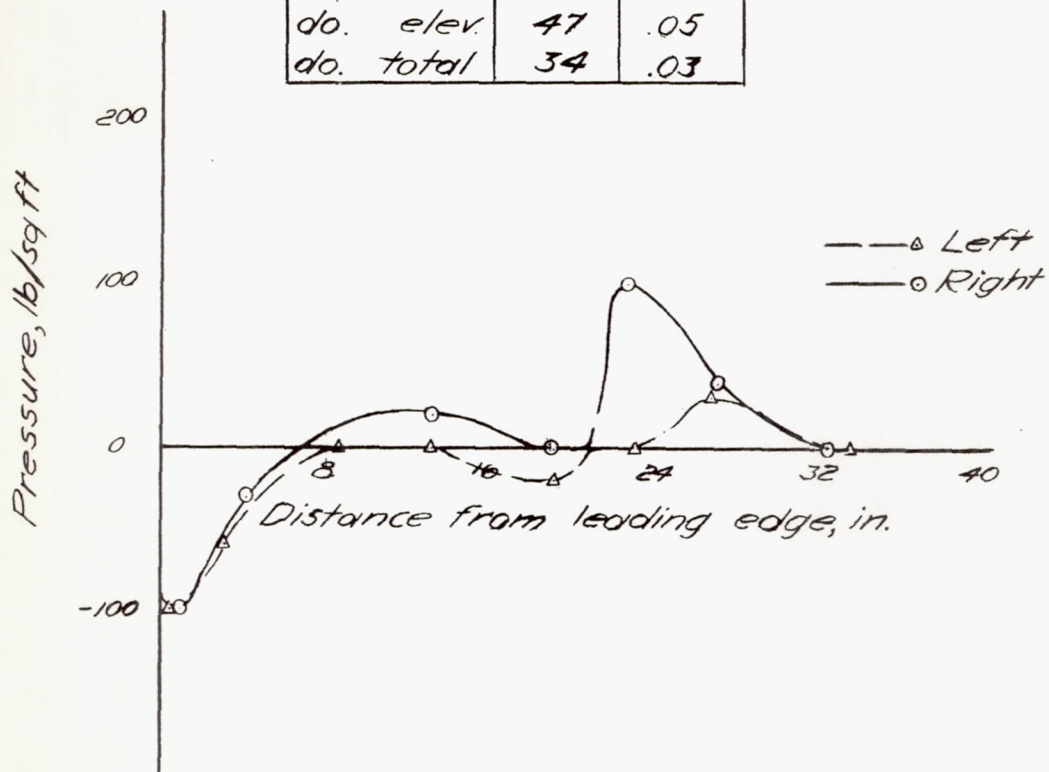


(c) Photographic prints of some of the records showing relative amount of buffeting during the run.

Figure 7.- (Concluded.)

$V_i = 345 \text{ mph}$
 $M = 0.722$
 Altitude 25,350ft

Chord	lb/ft	C_l
Left stab.	-42	-.05
do. elev.	17	.02
do. total	-25	-.03
Right stab.	-13	-.02
do. elev.	47	.05
do. total	34	.03



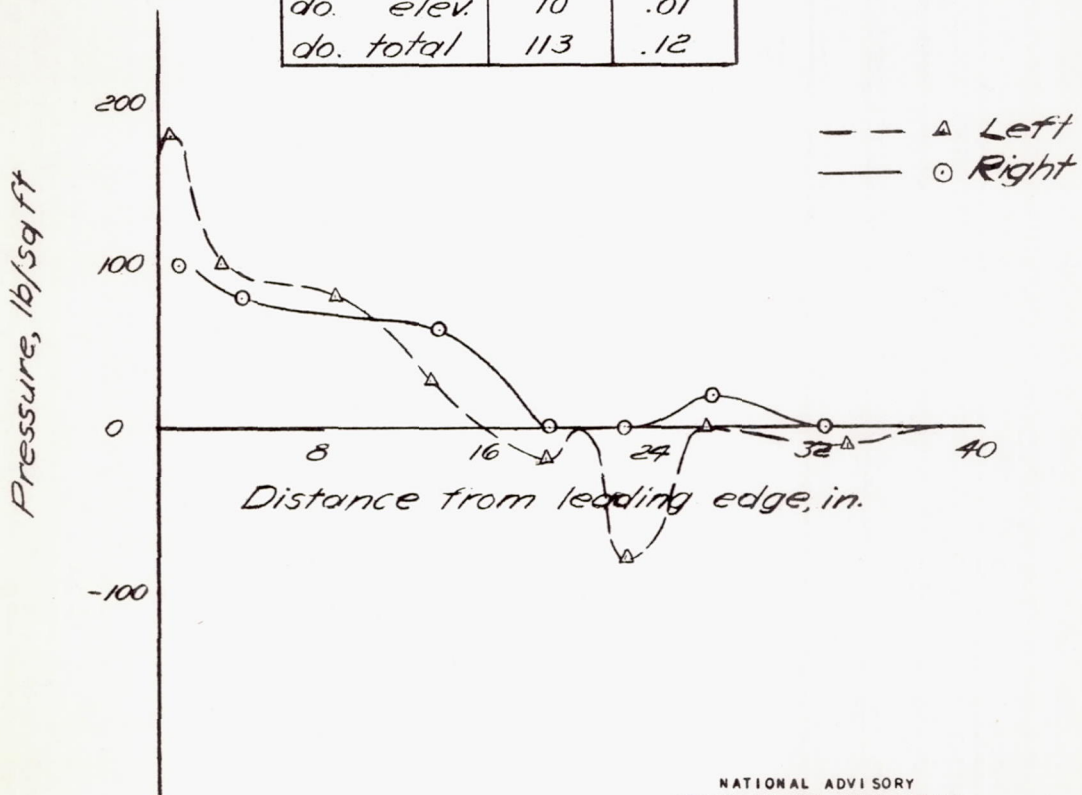
(a) At 3.0 seconds.

NATIONAL ADVISORY
COMMITTEE FOR AERONAUTICS

Figure 8. - Chordwise load distribution at 60 percent semispan in the dive pull-out shown in figure 7.

$V_i = 354 \text{ mph}$
 $M = 0.726$
 Altitude 24,450 ft

Chord	lb/ft	C_l
Left stab.	101	.11
do. elev.	-30	-.03
do. total	71	.08
Right stab.	103	.11
do. elev.	10	.01
do. total	113	.12



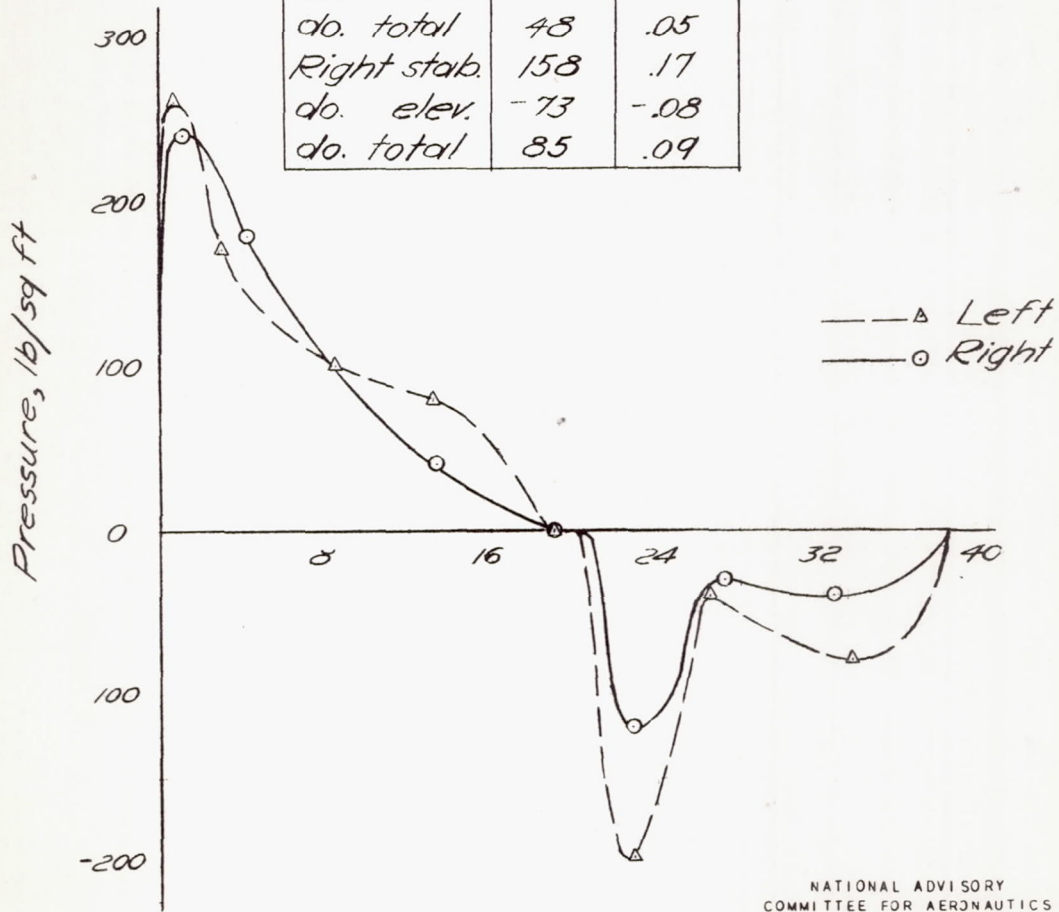
NATIONAL ADVISORY
COMMITTEE FOR AERONAUTICS

(b) At 4.0 seconds.

Figure 8. - Continued.

$V_i = 360 \text{ mph}$
 $M = 0.723$
 Altitude 23,300ft

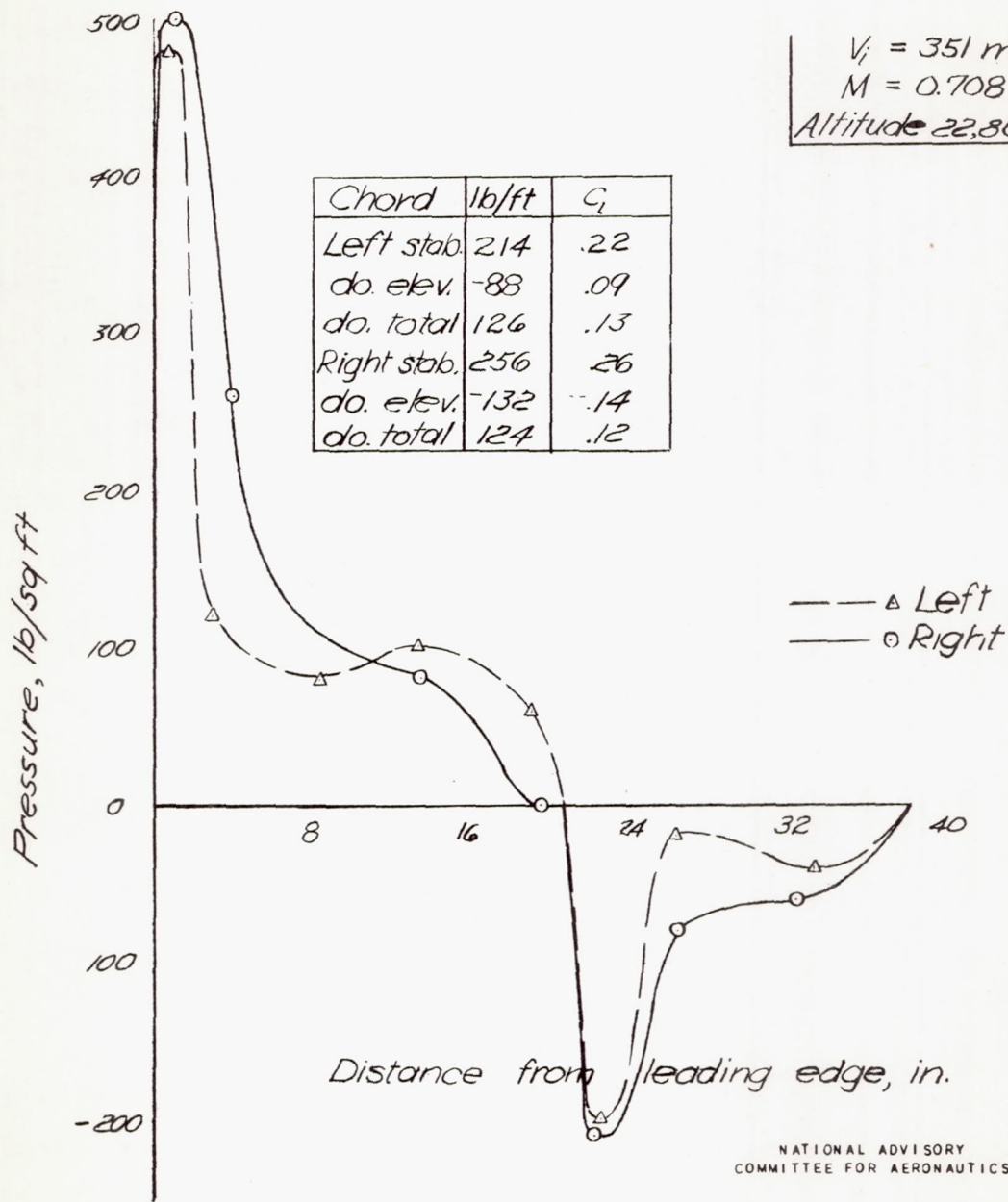
Chord	lb/ft	C_L
Left stab.	171	.18
do. elev.	-123	-.13
do. total	48	.05
Right stab.	158	.17
do. elev.	-73	-.08
do. total	85	.09



NATIONAL ADVISORY
COMMITTEE FOR AERONAUTICS

(c) At 6.0 seconds.

Figure 8. - Continued.



(d) At 7.5 seconds.

Figure 8 - Concluded

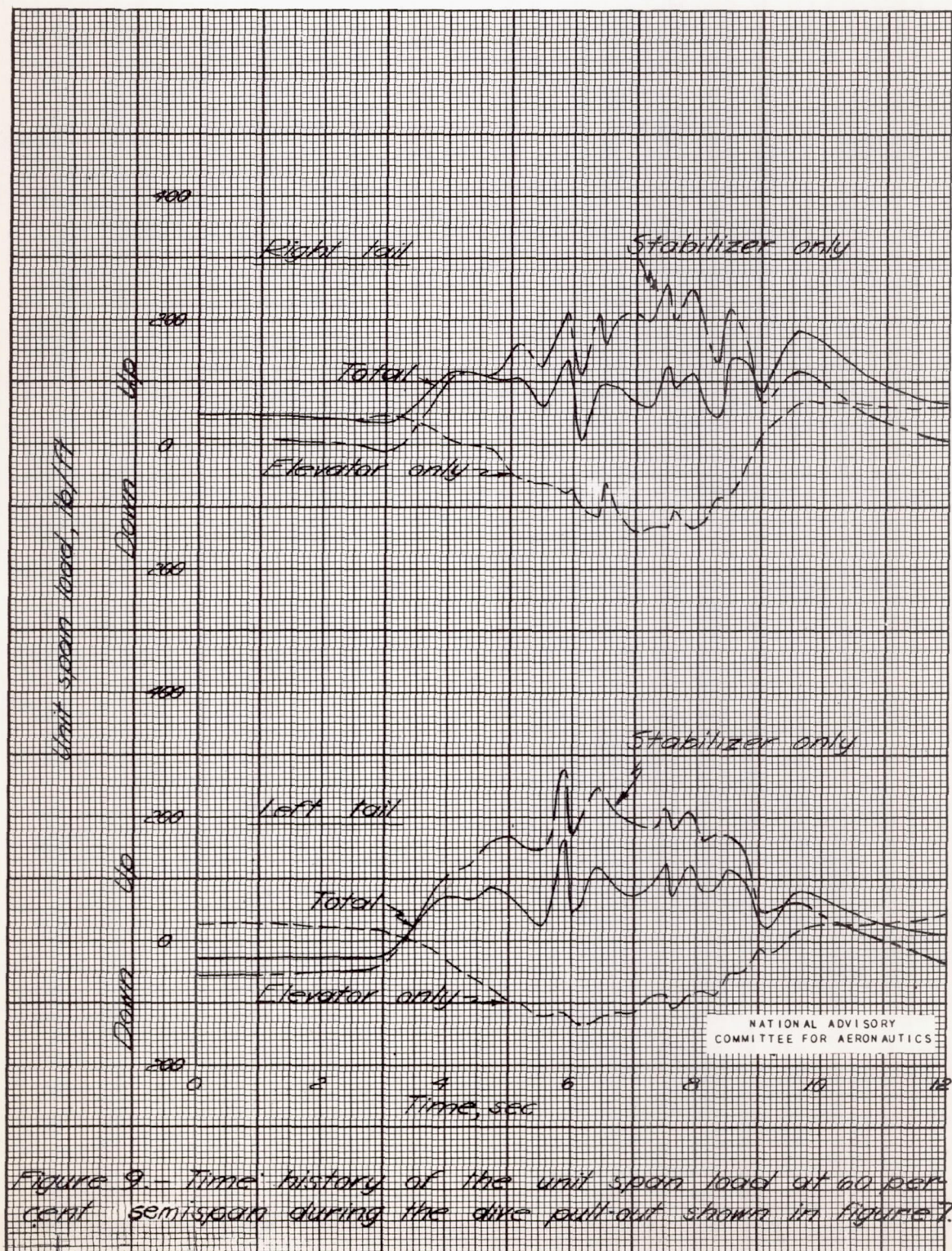
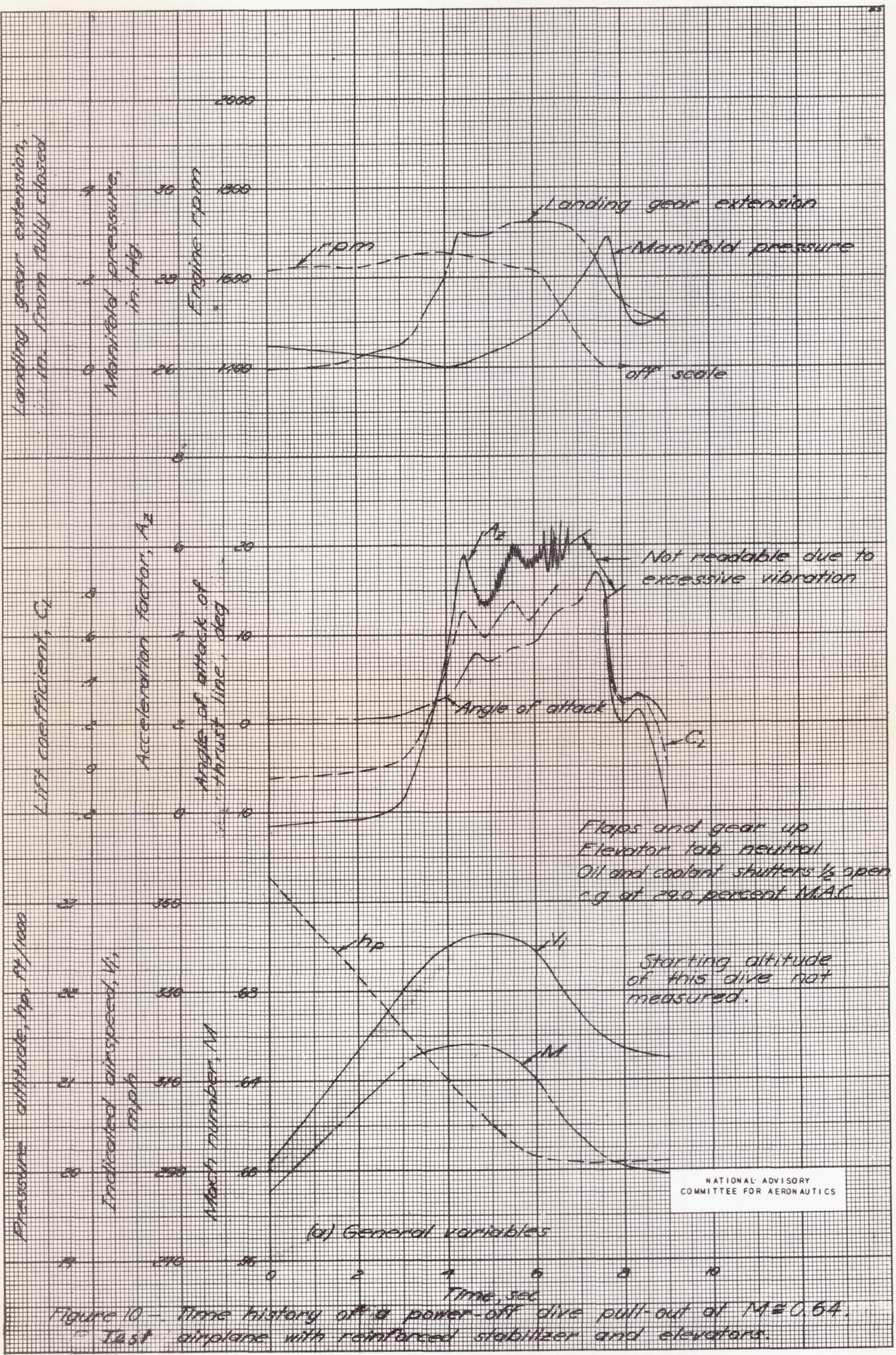


Figure 9.- Time history of the unit span load at 60 per cent semispan during the dive pull-out shown in figure 7.



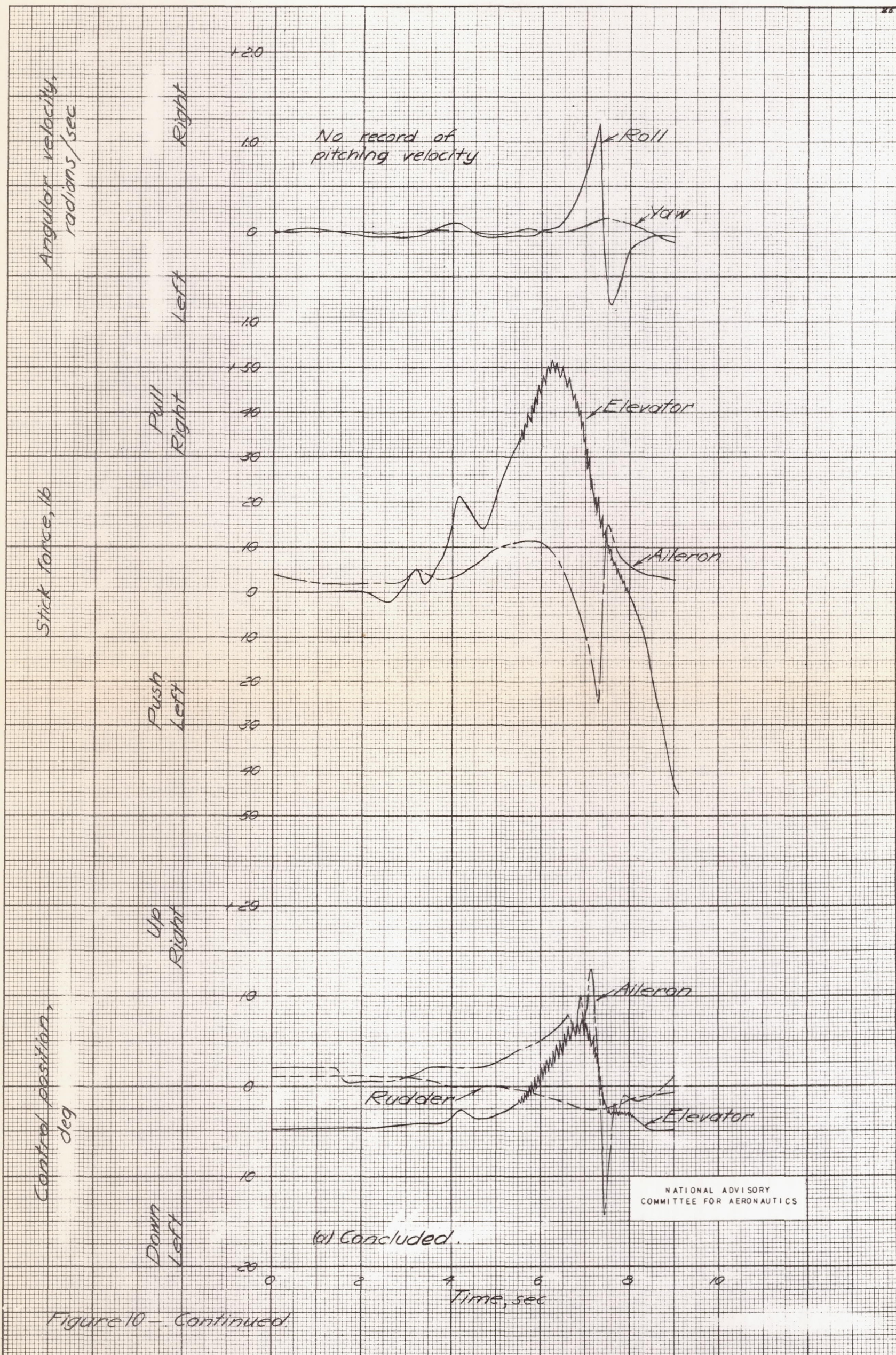
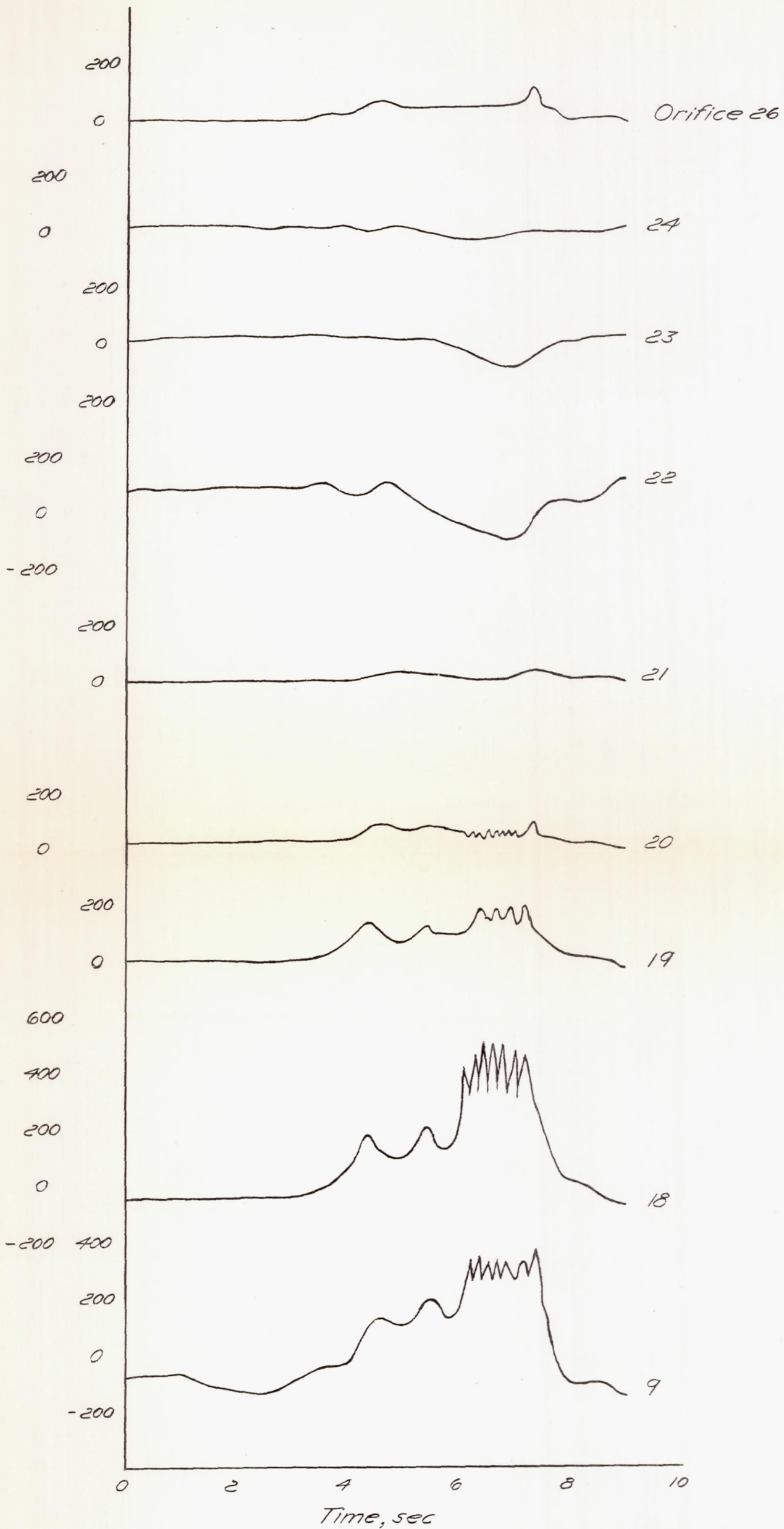


Figure 10 - Continued

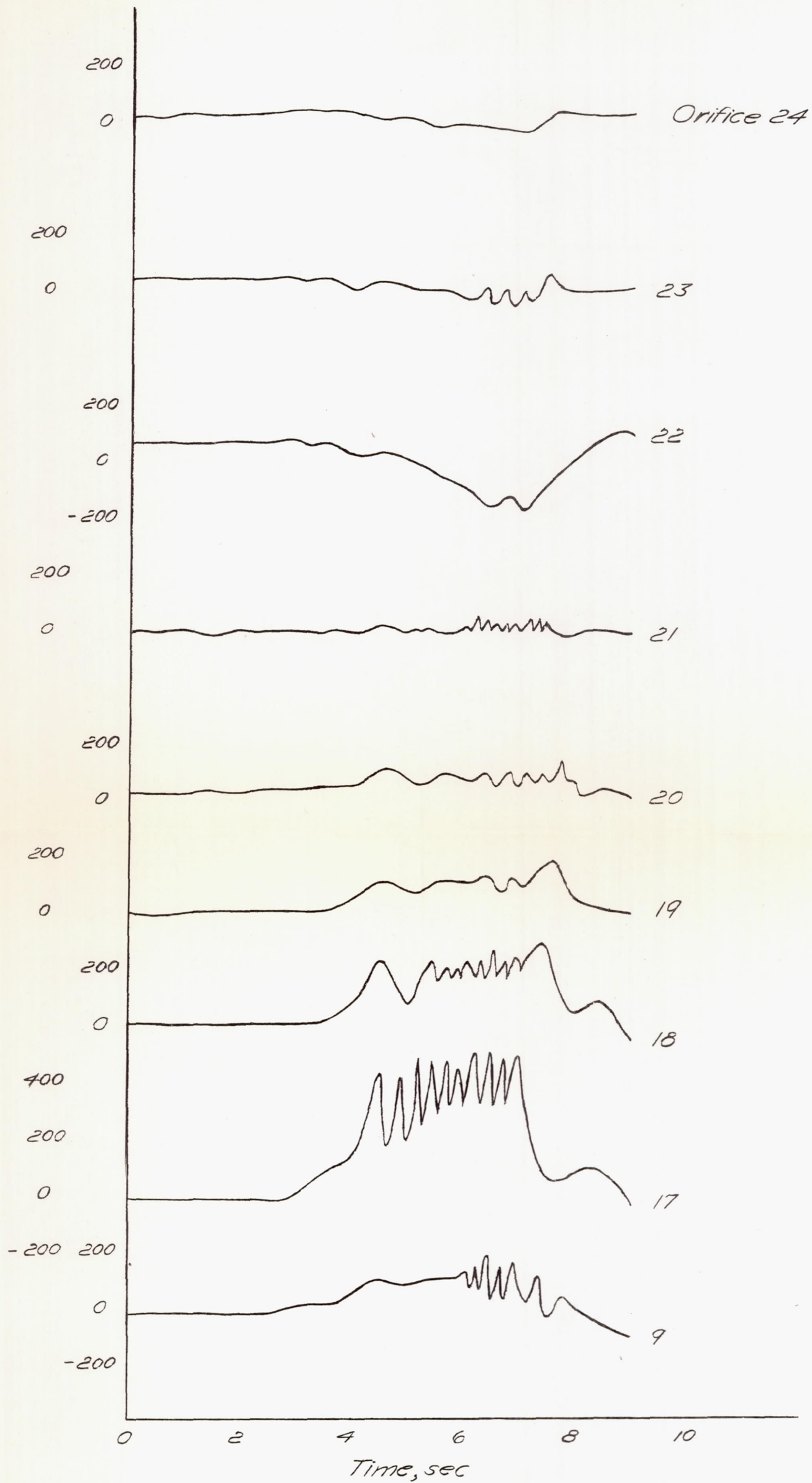
Pressures on right tail, lb/sq ft



(b) Tail pressures.

Figure 10. - Continued.

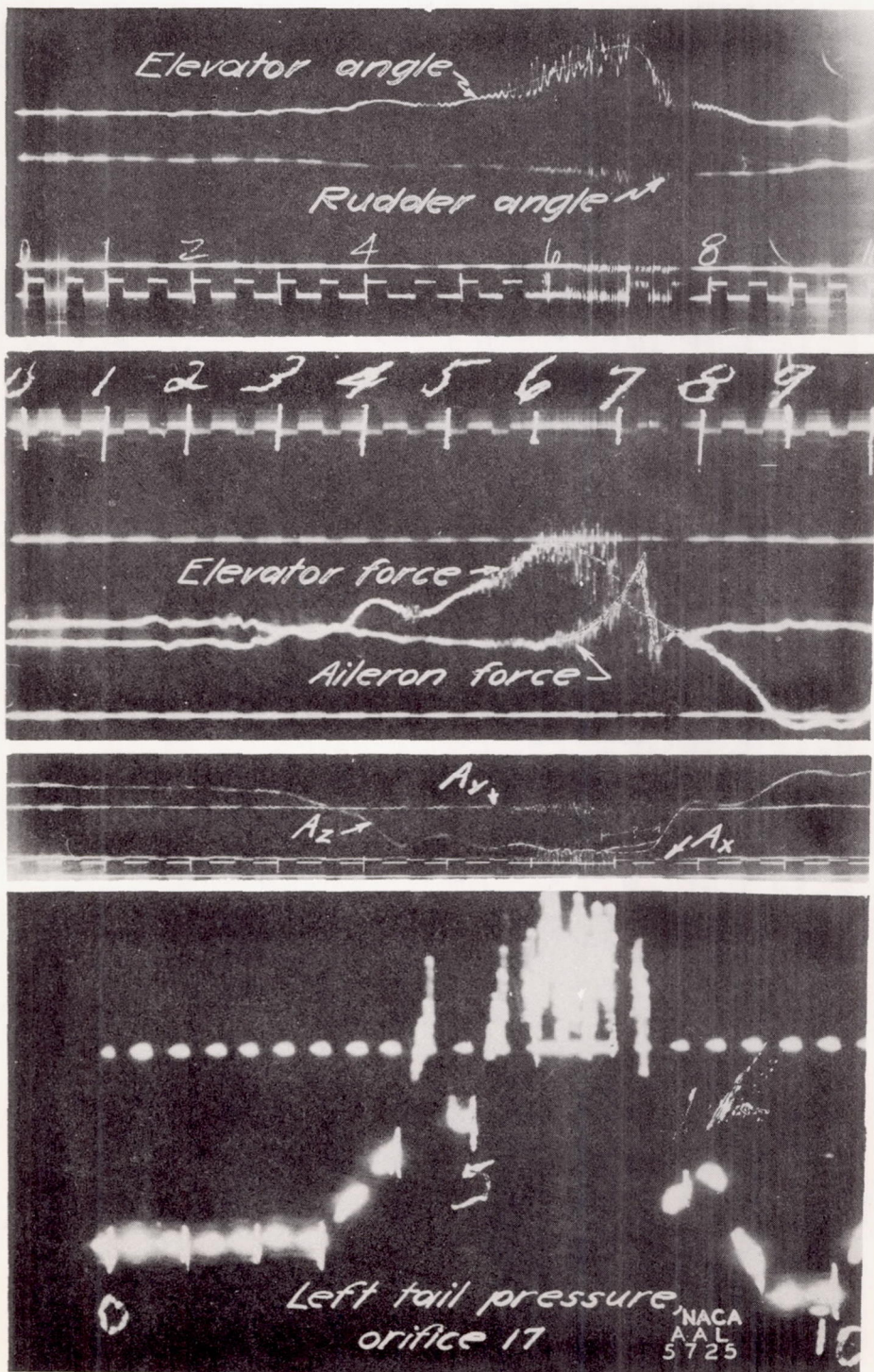
Pressures on left tail, lb/sq ft



(b) Concluded.

NATIONAL ADVISORY
COMMITTEE FOR AERONAUTICS

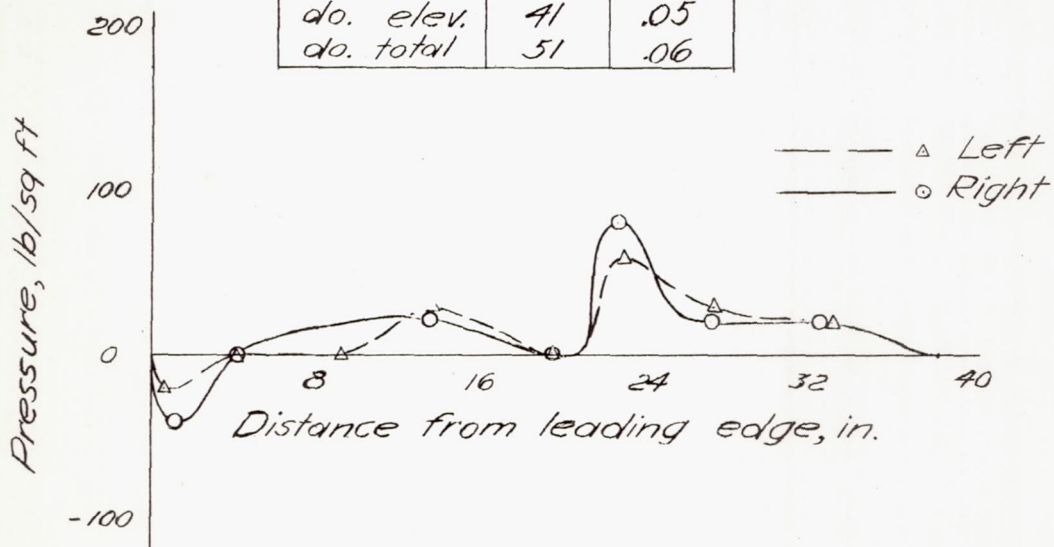
Figure 10. - Continued.



(c) Photographic prints of some of the records showing relative amount of buffeting during the run.

$V_i = 317 \text{ mph}$
 $M = 0.629$
 Altitude 22,200 ft

Chord	lb/ft	C_L
Left stab.	11	.01
do. elev.	40	.05
do. total	51	.06
Right stab.	10	.01
do. elev.	41	.05
do. total	51	.06



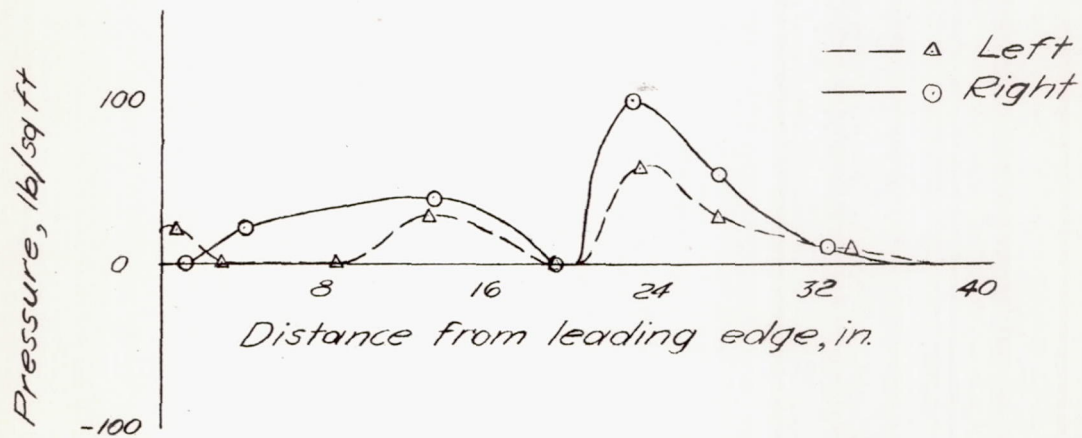
(a) At 2.0 seconds.

NATIONAL ADVISORY
COMMITTEE FOR AERONAUTICS

Figure 11. - Chordwise load distribution at 60 percent semispan in the dive pull-out shown in figure 10.

$V_i = 330 \text{ mph}$
 $M = 0.653$
 Altitude 21,300 ft

Chord	lb/ft	C_l
Left stab.	30	.04
do. elev.	37	.04
do. total	67	.08
Right stab.	44	.05
do. elev.	61	.08
do. total	105	.13



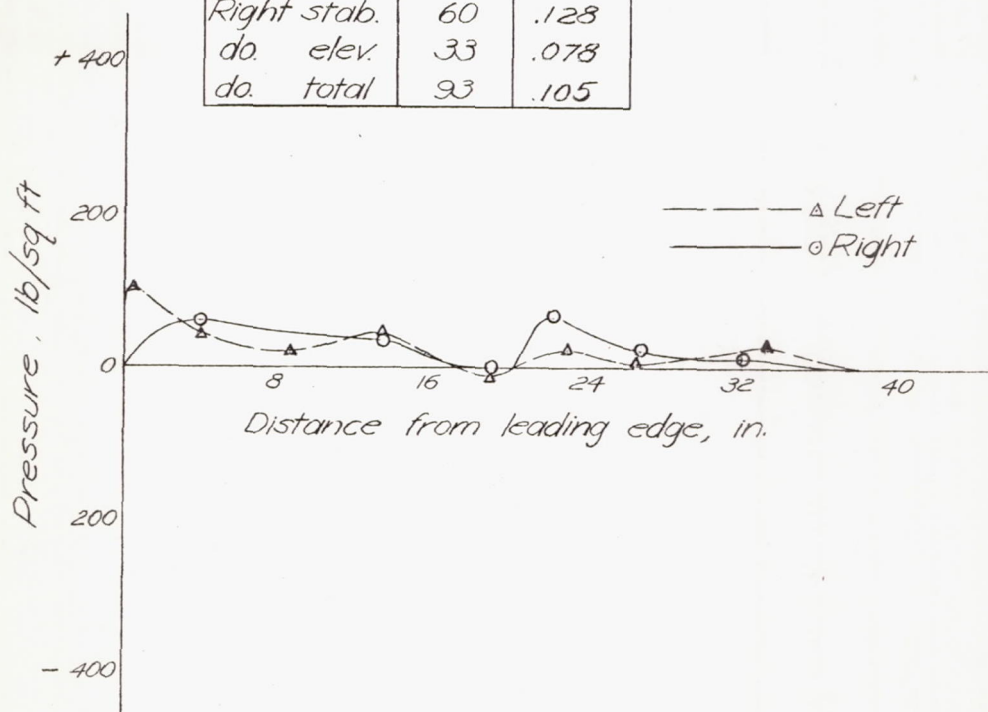
NATIONAL ADVISORY
 COMMITTEE FOR AERONAUTICS

(b) At 3.5 seconds.

Figure 11. - Continued.

$V_i = 339 \text{ mph}$
 $M = 0.656$
Altitude = 21,050 ft

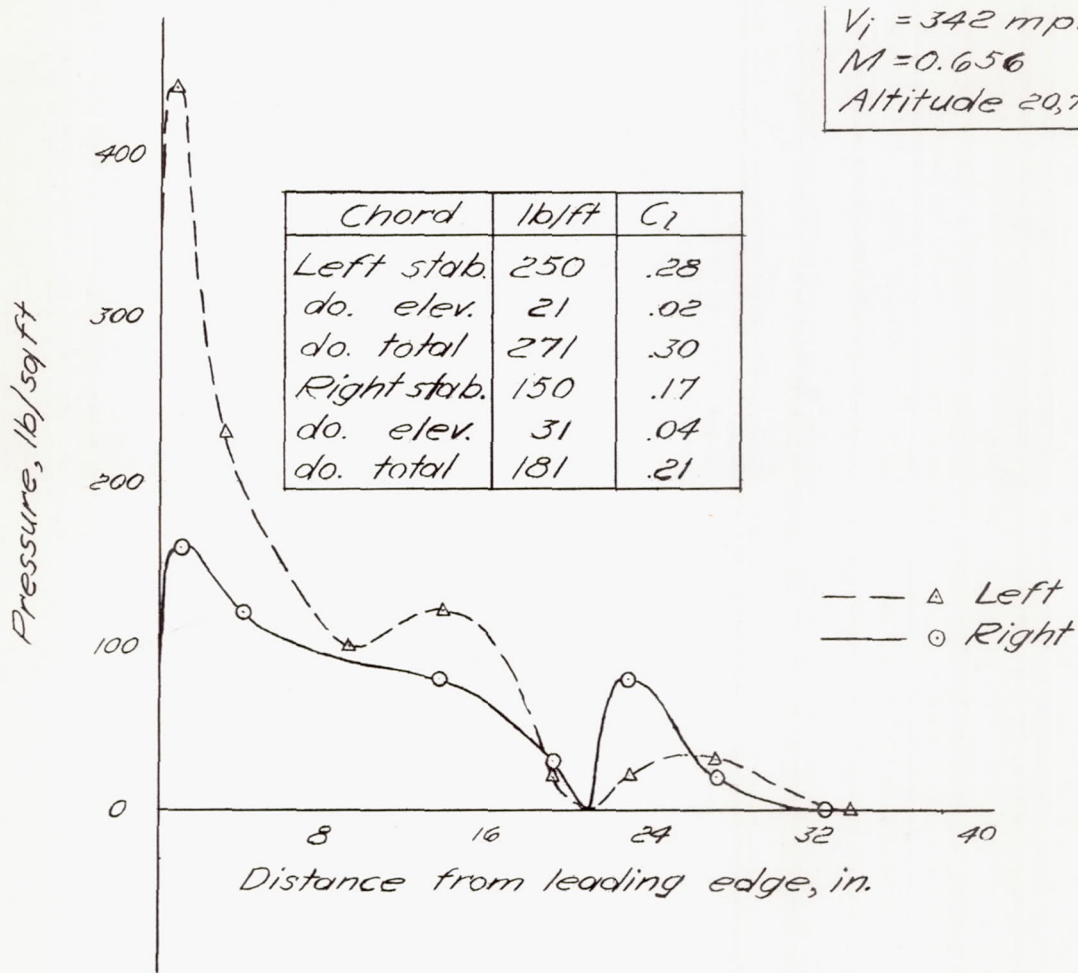
Chord	lb/ft	C_l
Left stab.	55	.117
do. elev.	20	.043
do. total	75	.085
Right stab.	60	.128
do. elev.	33	.078
do. total	93	.105



(c) At 3.9 seconds

Figure 11.- Continued

NATIONAL ADVISORY
COMMITTEE FOR AERONAUTICS



NATIONAL ADVISORY
COMMITTEE FOR AERONAUTICS

(d) At 4.5 seconds.

Figure 11. - Continued.

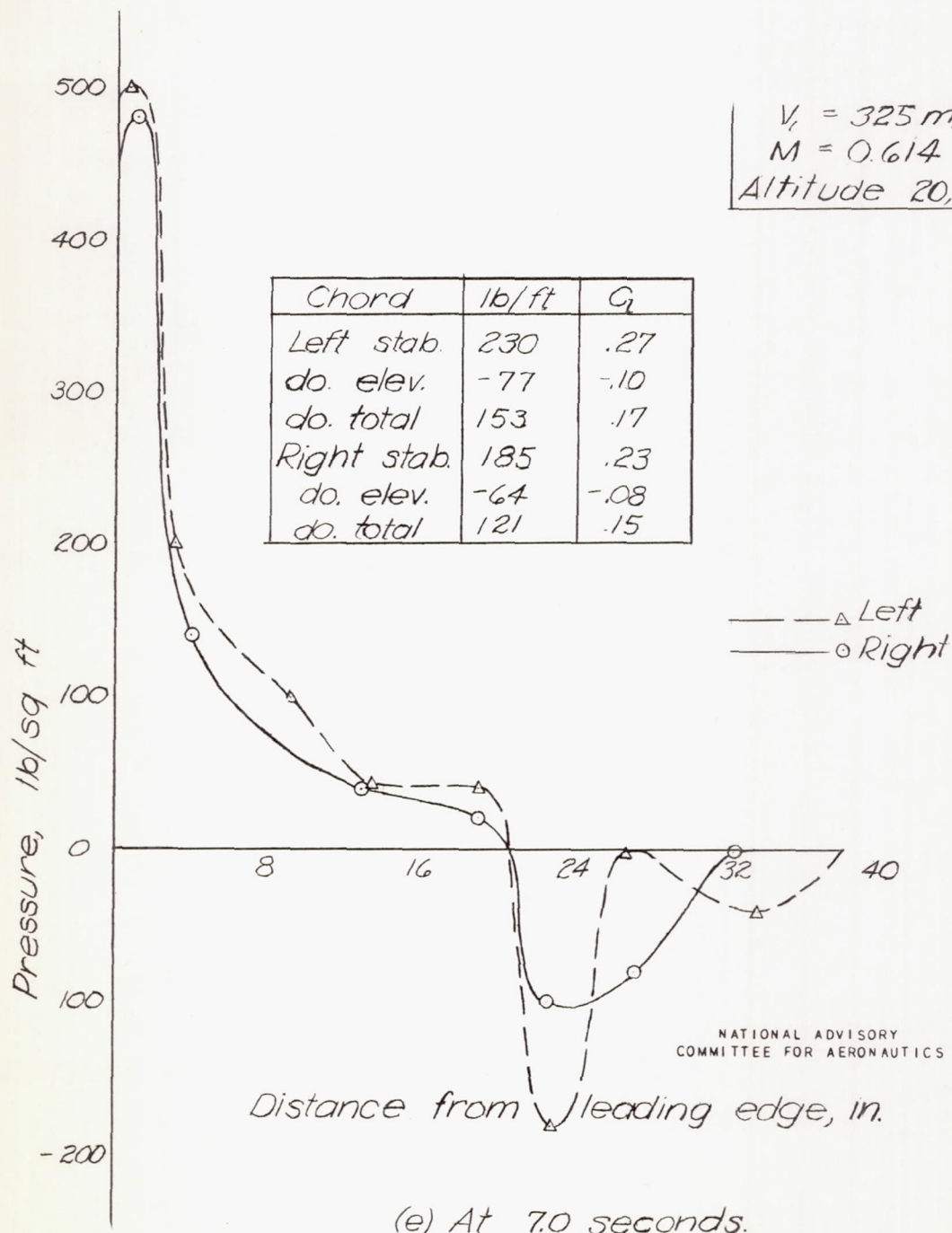
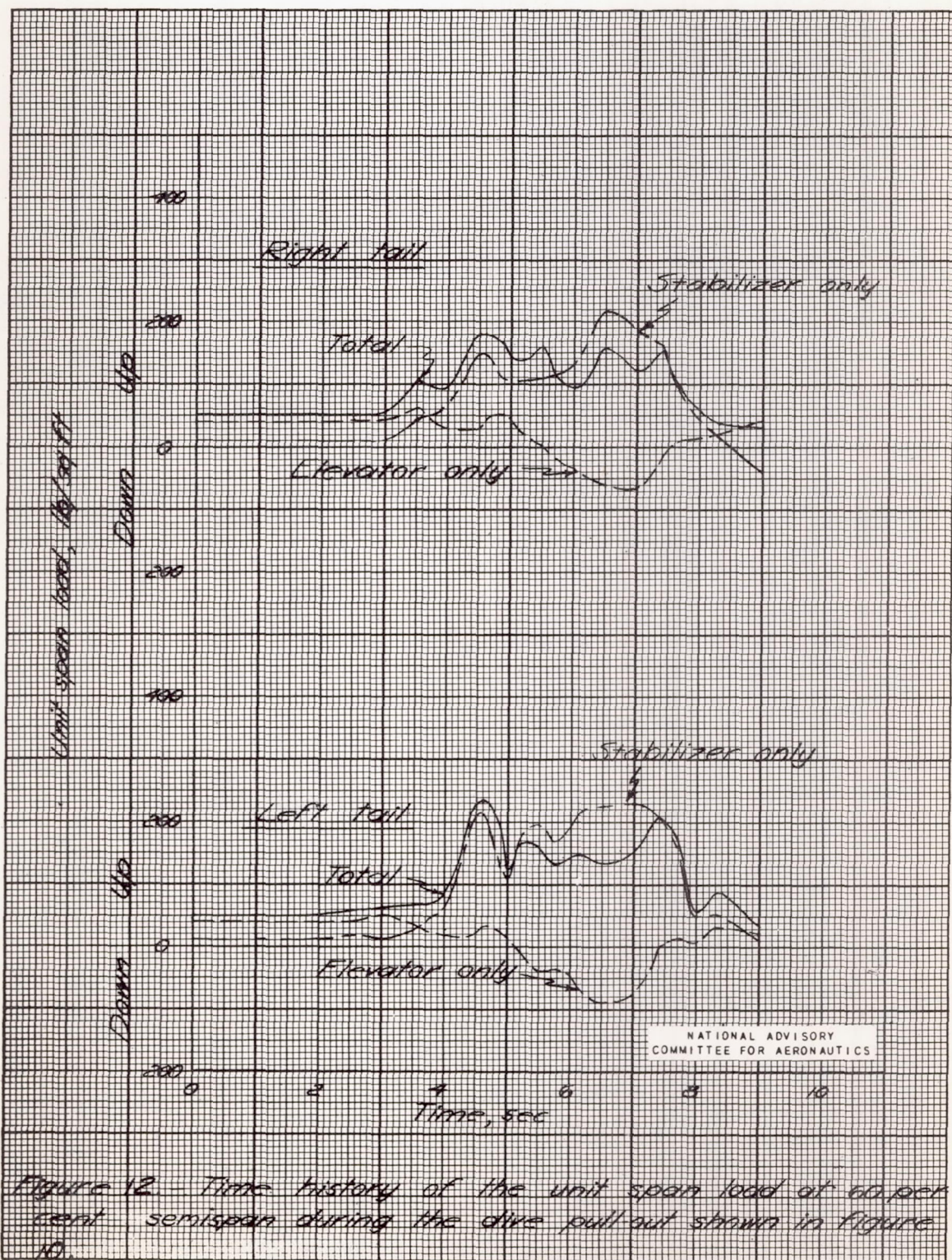
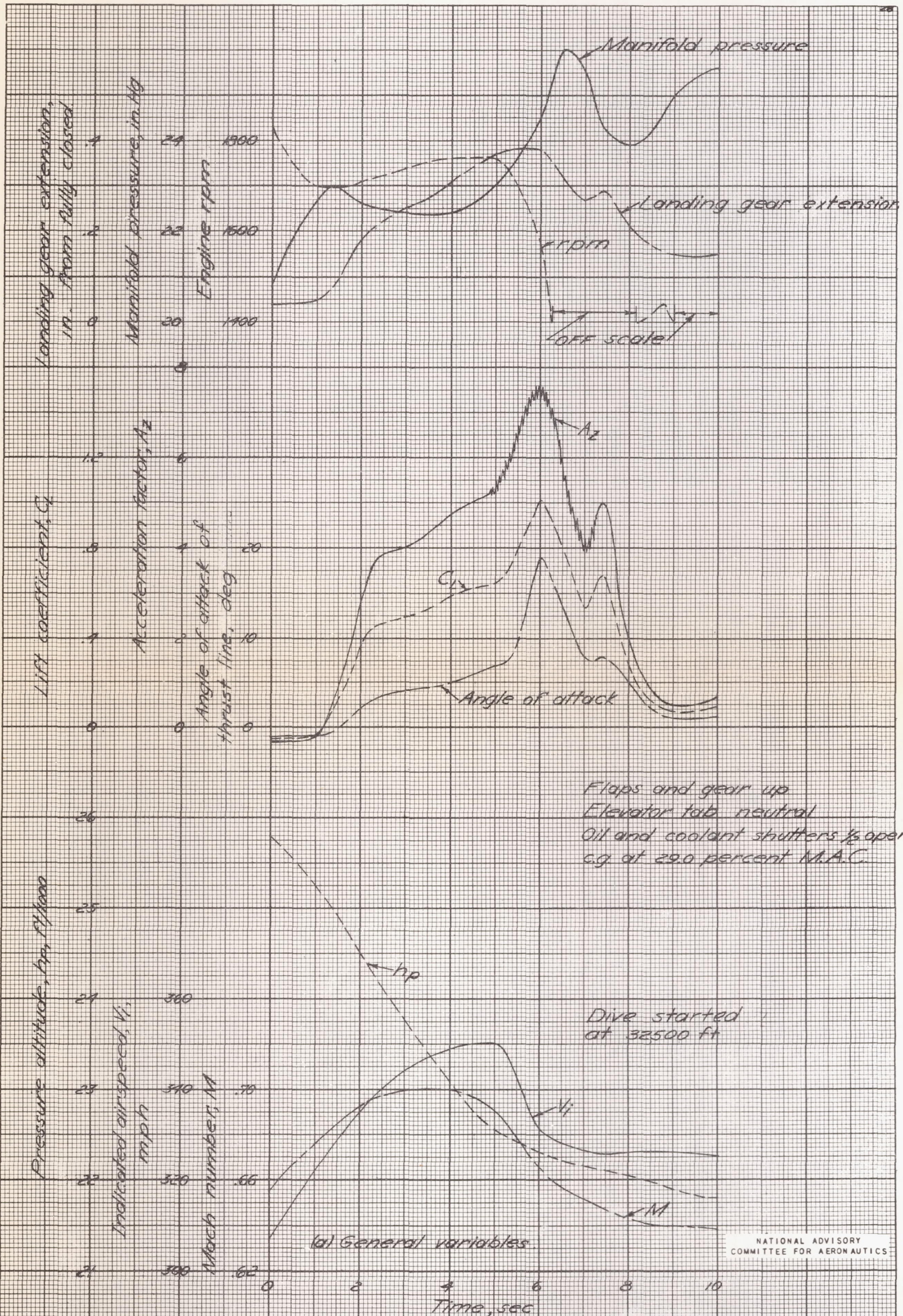


Figure 11. - Concluded.



NATIONAL ADVISORY
COMMITTEE FOR AERONAUTICS

Figure 12. Time history of the unit span load at 60 per cent semispan during the dive pull-out shown in figure 10.



NATIONAL ADVISORY
COMMITTEE FOR AERONAUTICS

Figure 13 - Time history of a power-off dive pull-out at $M \approx 0.67$ in which partial failure of the reinforced horizontal tail structure occurred.

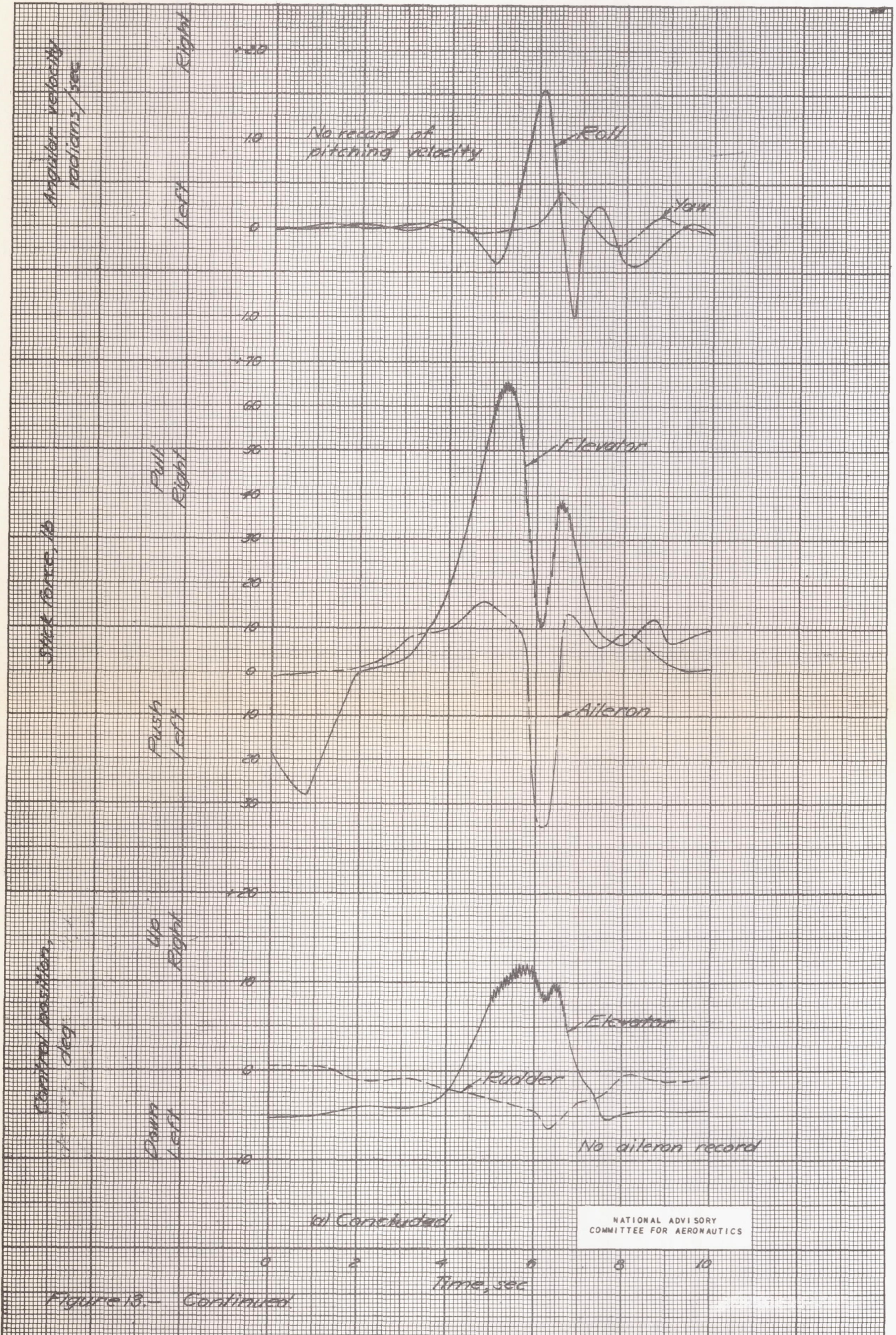
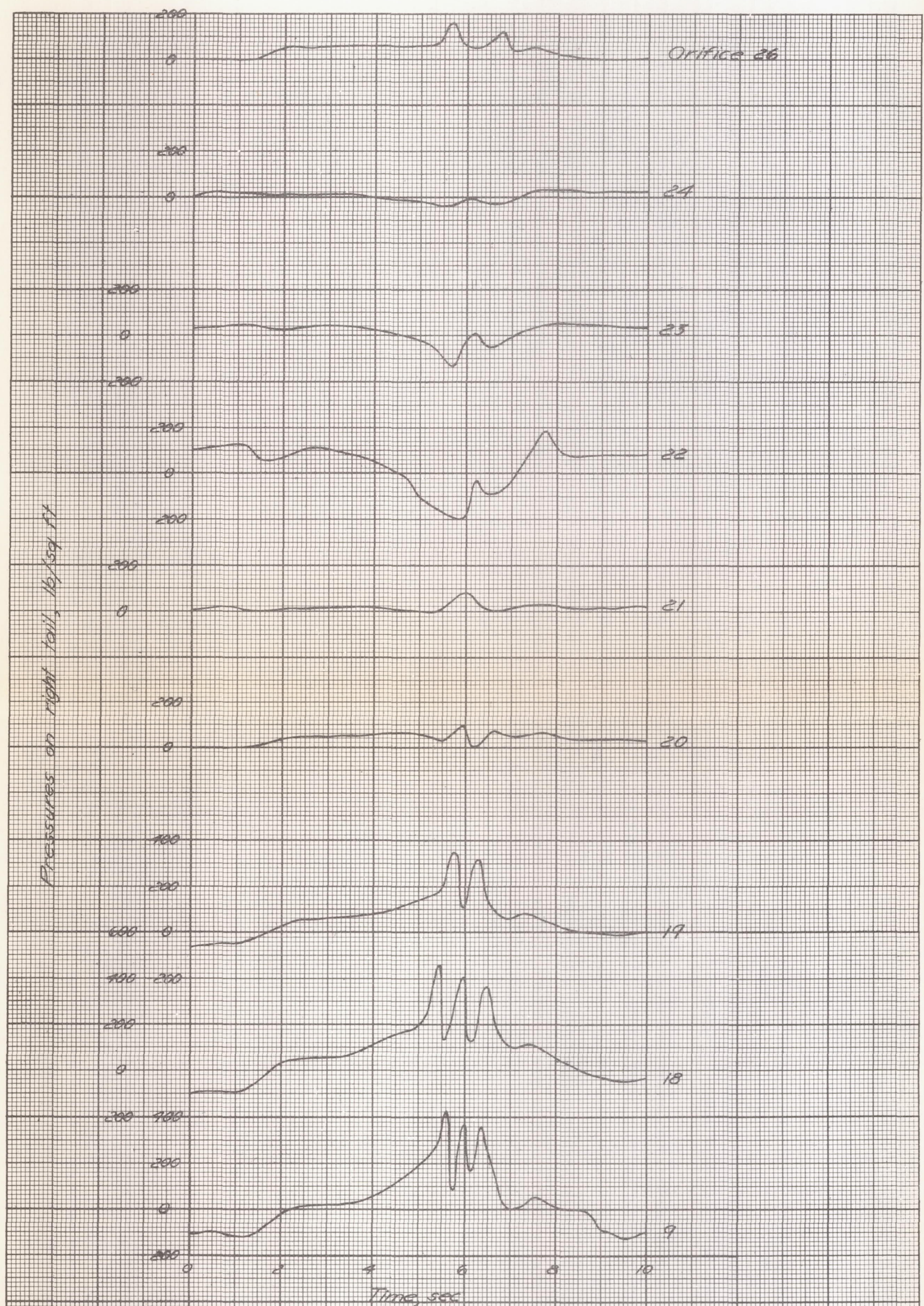


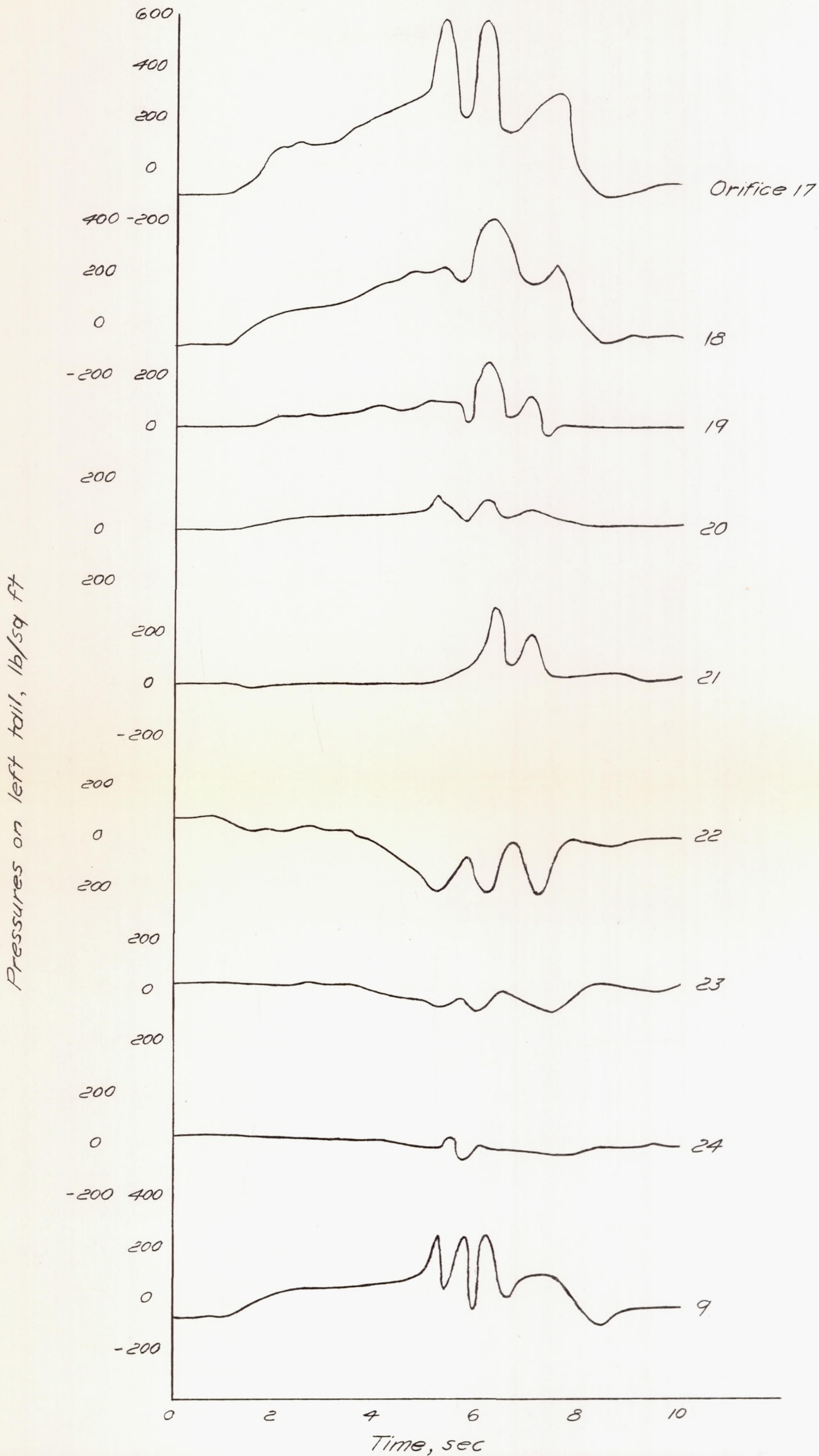
Figure 13.- Continued

NATIONAL ADVISORY COMMITTEE FOR AERONAUTICS



(b) Tail pressures.
Figure 13. - Continued

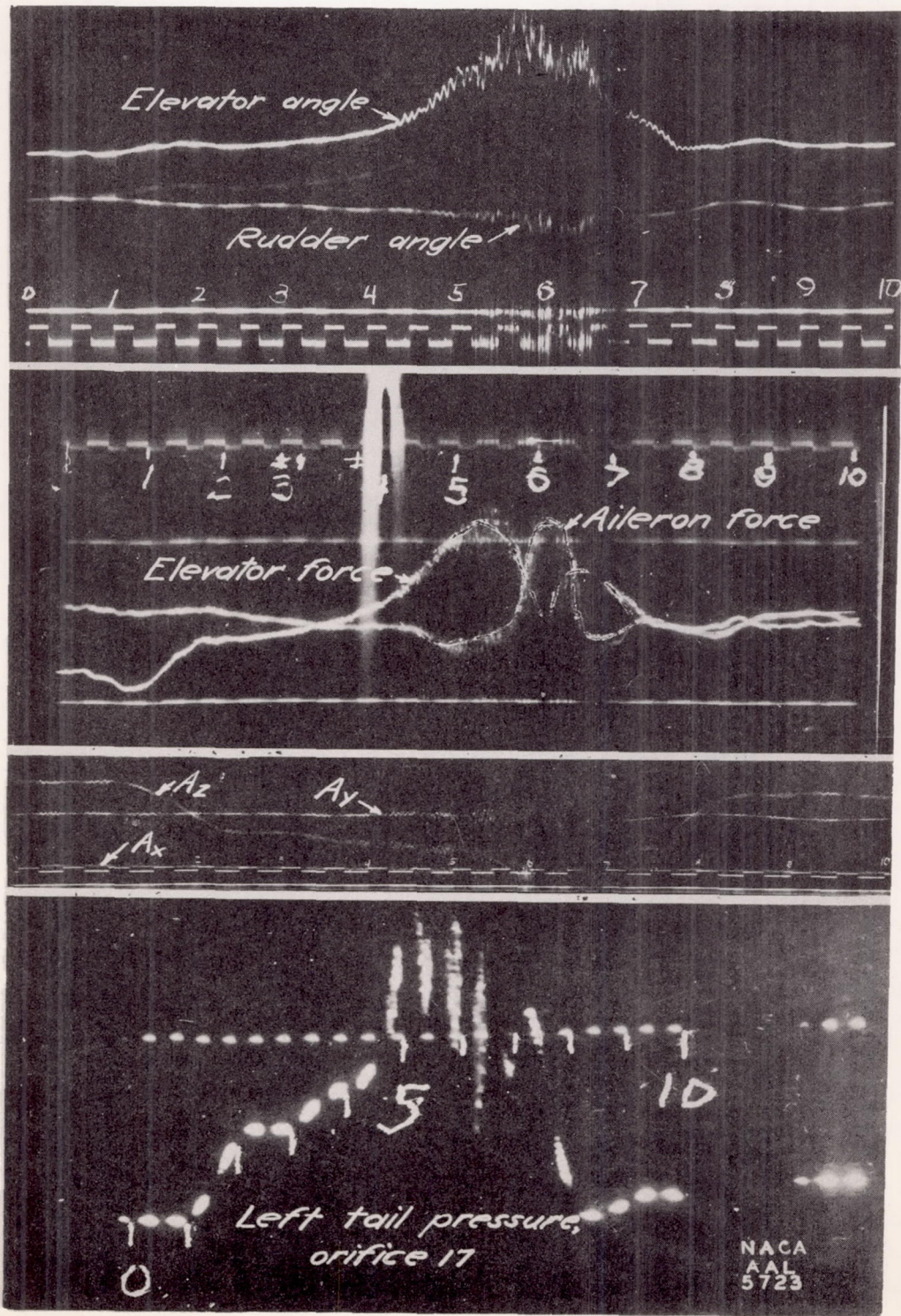
NATIONAL ADVISORY
COMMITTEE FOR AERONAUTICS



(b) Concluded.

NATIONAL ADVISORY
COMMITTEE FOR AERONAUTICS

Figure 13. - Continued.



(c) Photographic prints of some of the records showing relative amount of buffeting during the run.

Chord	lb/ft	C_l
Left stab.	-39	-.06
do. elev.	52	.07
do. total	13	.01
Right stab.	-45	-.06
do. elev.	48	.07
do. total	3	.01

$V_i = 307$
 $M = 0.656$
Altitude 25,800ft

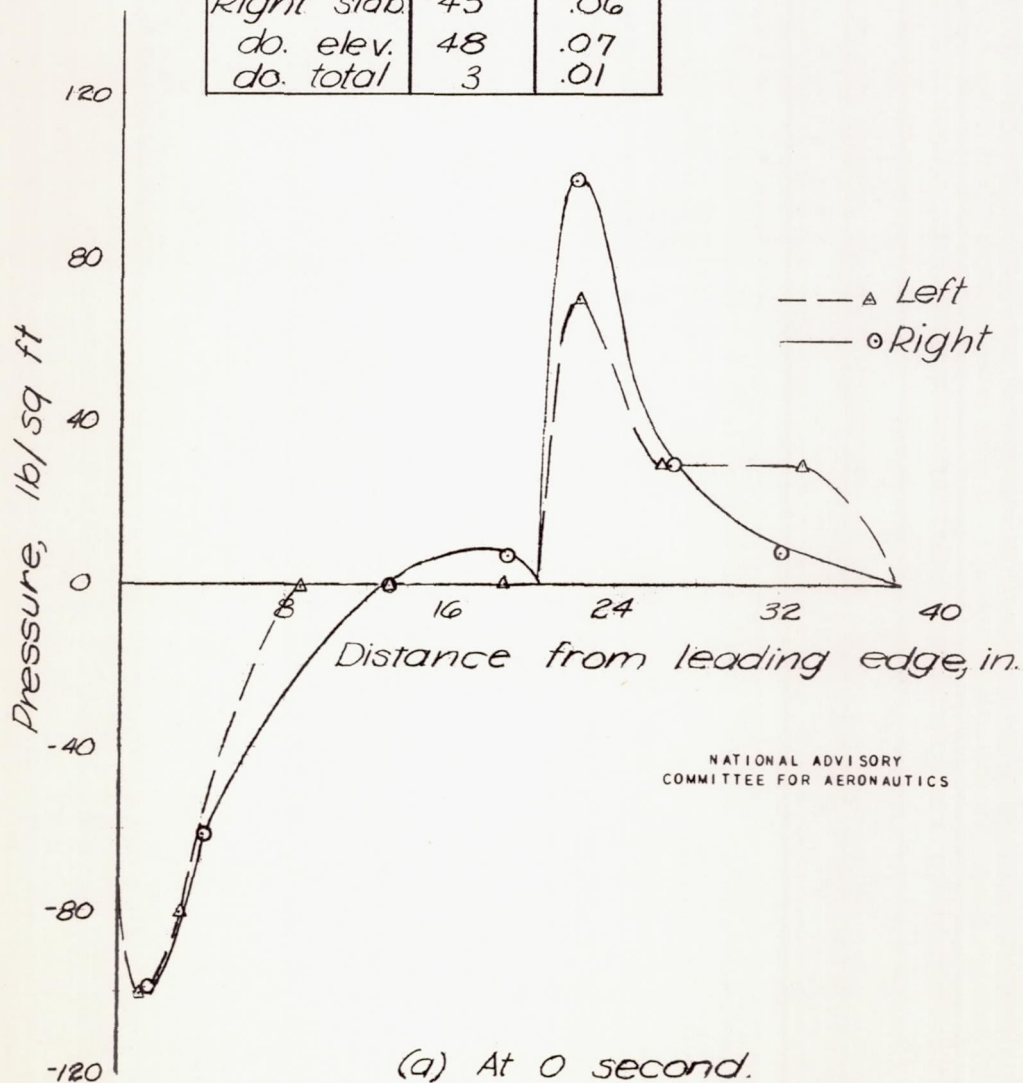
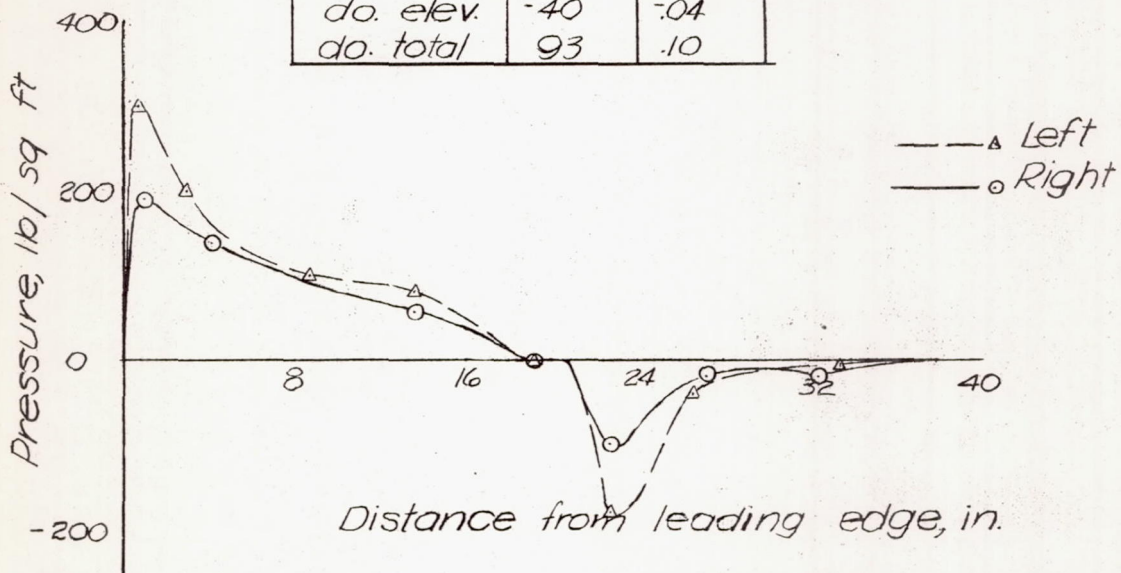


Figure 14. - Chordwise load distribution at 60 percent of semispan in the dive pull-out shown in figure 13.

$V_i = 350 \text{ mph}$
 $M = 0.691$
Altitude 22,500ft

Chord	lb/ft	C_L
Left stab.	173	.19
do. elev.	-71	-.08
do. total	102	.11
Right stab.	133	.14
do. elev.	-40	-.04
do. total	93	-.10



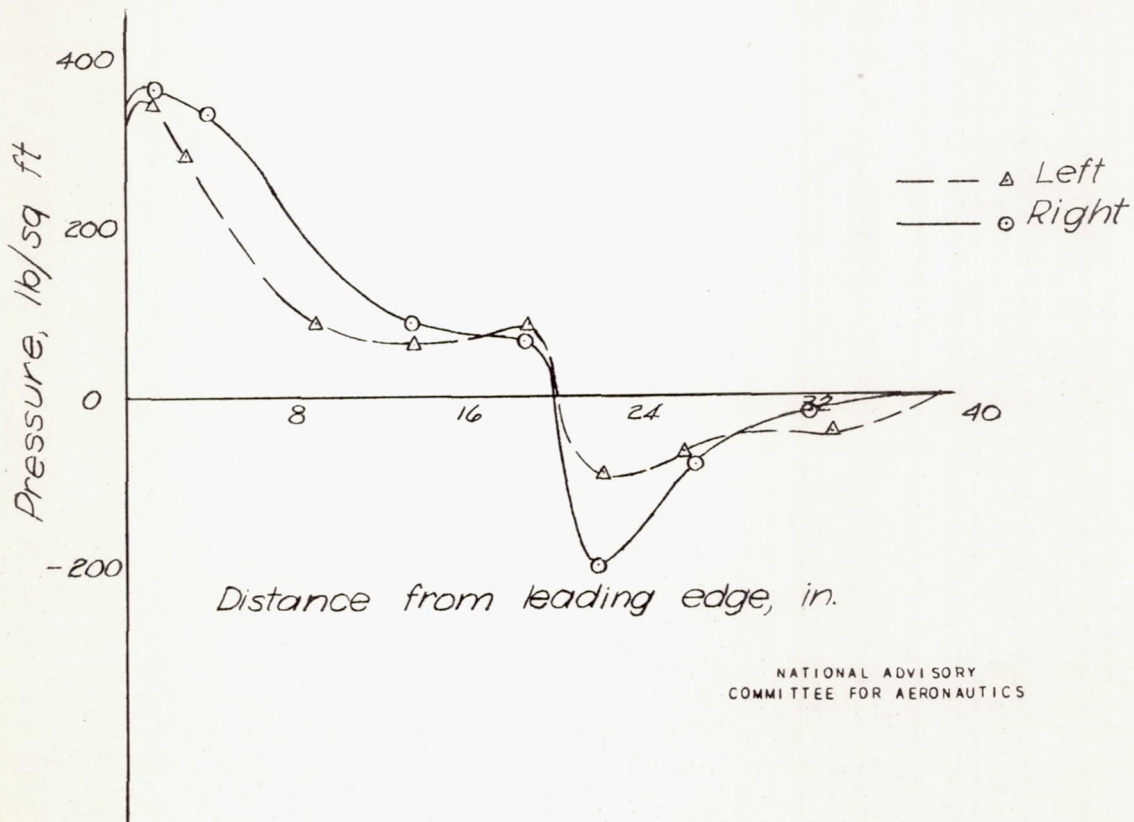
NATIONAL ADVISORY
COMMITTEE FOR AERONAUTICS

(b) At 5.0 seconds.

Figure 14.- Continued.

$V_i = 336 \text{ mph}$
 $M = 0.670$
 Altitude 23,500ft

Chord	lb/ft	C_l
Left stab.	227	.26
do. elev.	-79	-.09
do. total	148	.17
Right stab.	308	.36
do. elev.	-118	-.14
do. total	190	.22



NATIONAL ADVISORY
COMMITTEE FOR AERONAUTICS

(c) At 5.9 seconds.

Figure 14.- Concluded.

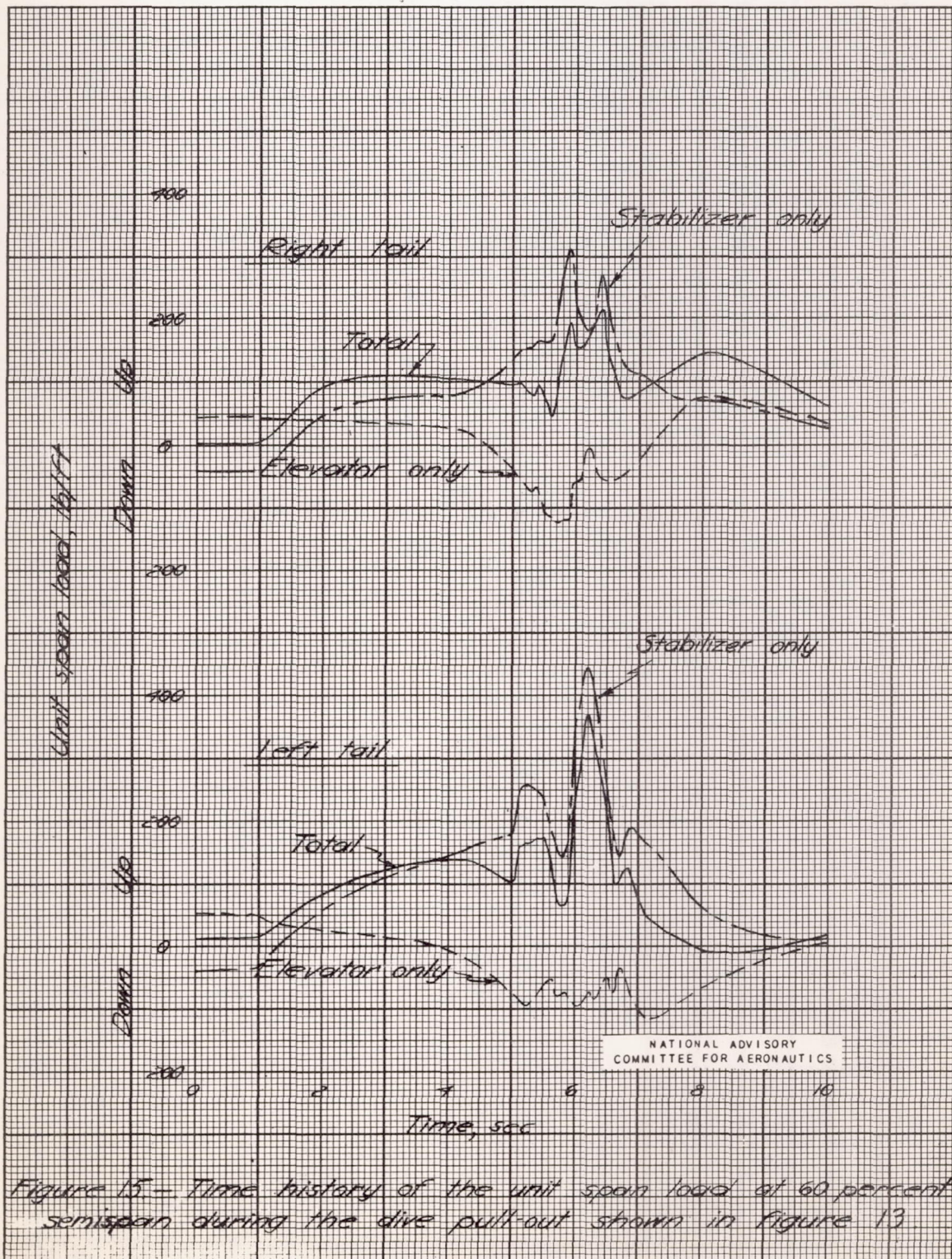


Figure 15 - Time history of the unit span load at 60 percent semispan during the dive pull-out shown in figure 13

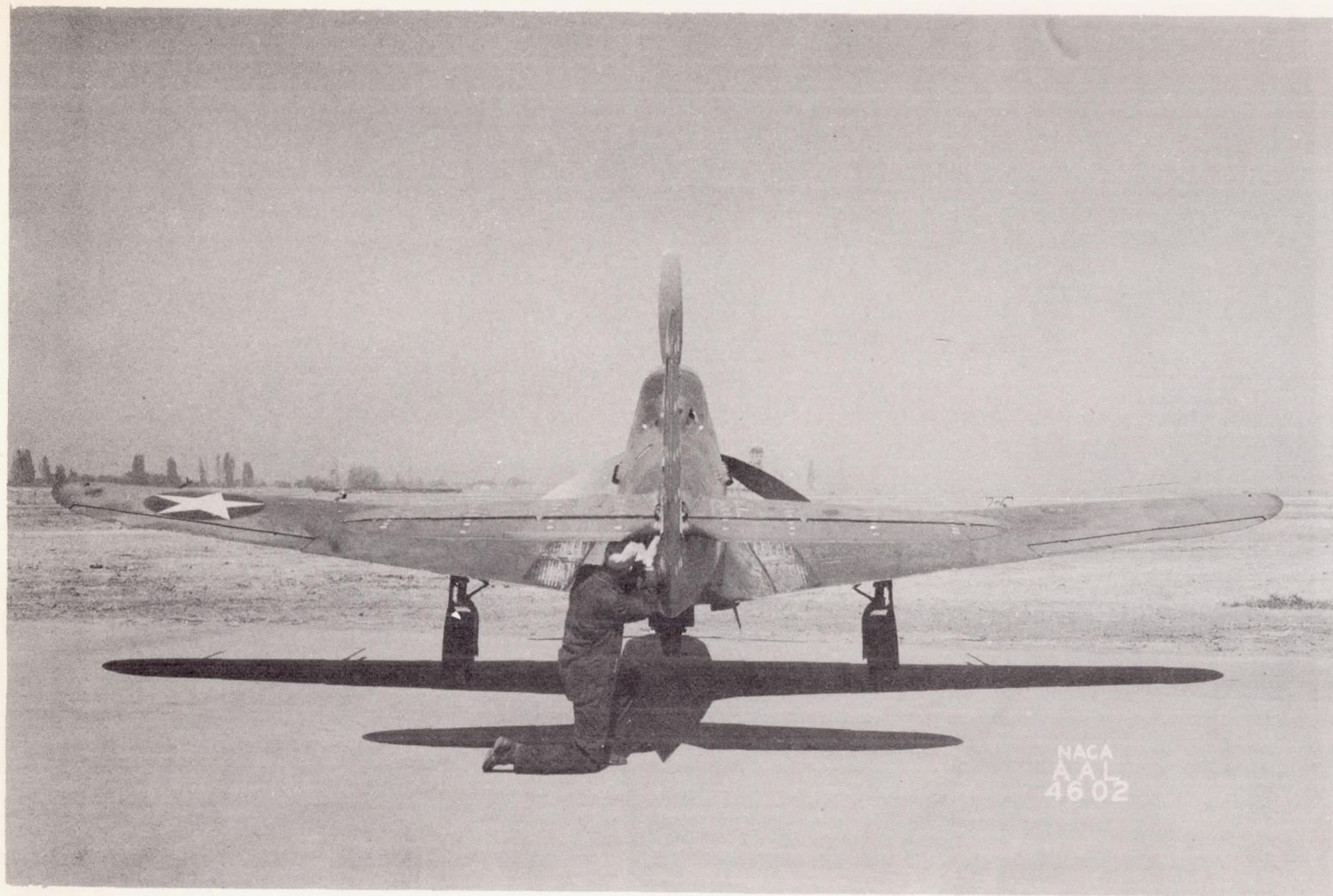


Figure 16.- Rear view, test airplane as instrumented for tail-load flight tests, showing undamaged tail surfaces.



Figure 17.- Rear view showing damaged horizontal tail surfaces.

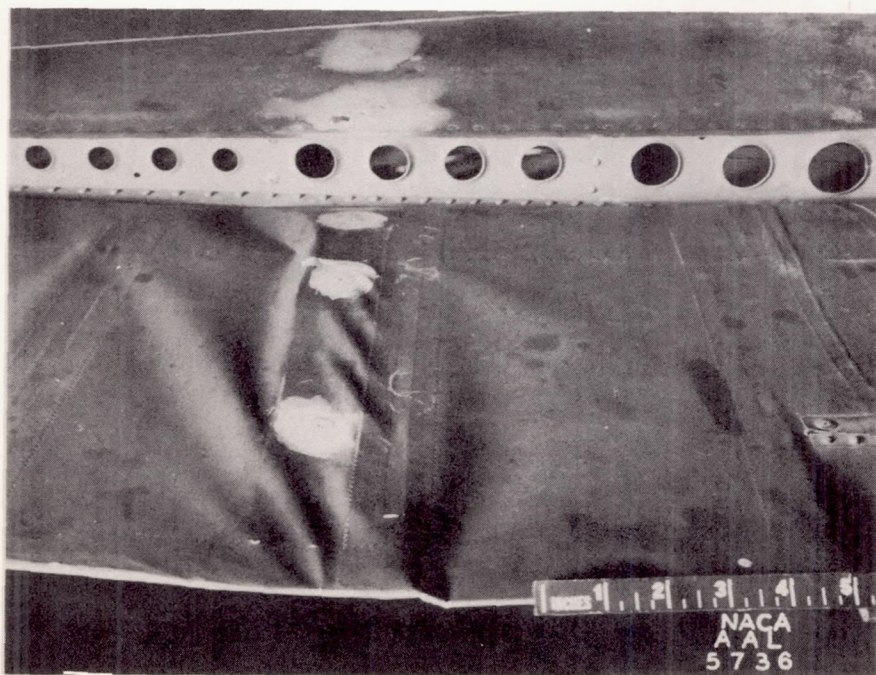


Figure 18.- Rear view of the buckled left elevator.

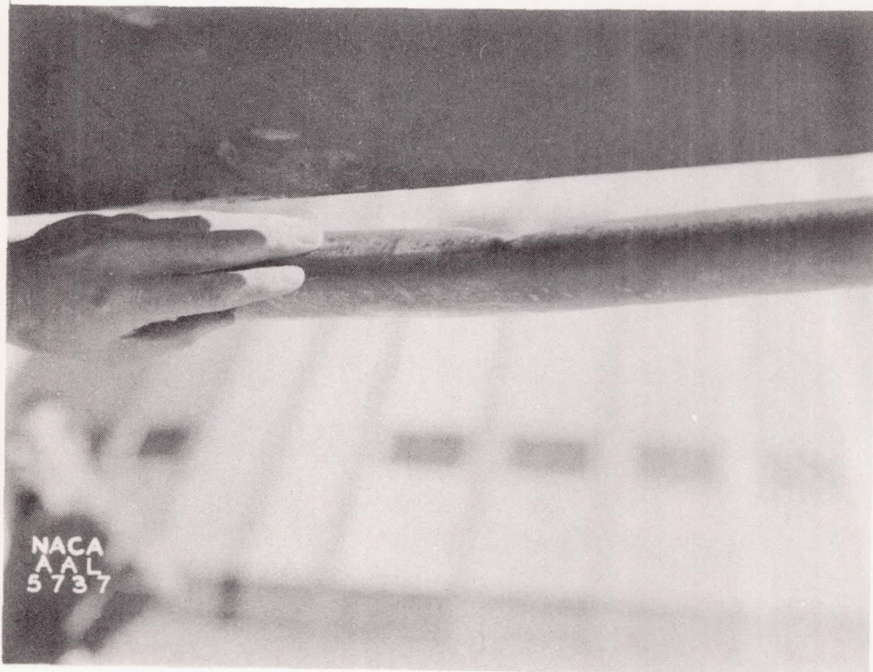


Figure 19.- Lower front view of the buckled left elevator.

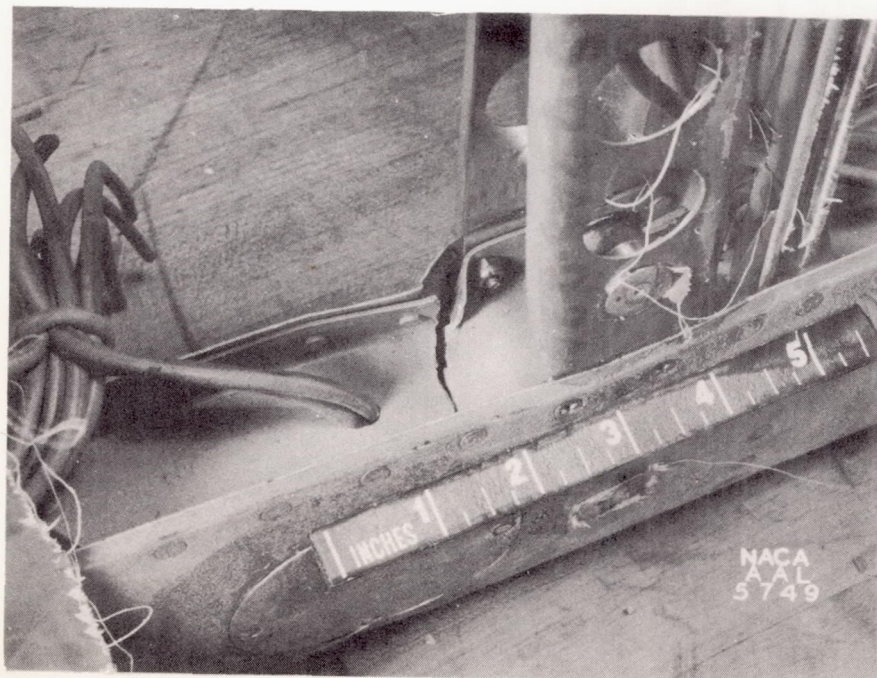


Figure 20.- Detail of cracked elevator spar.

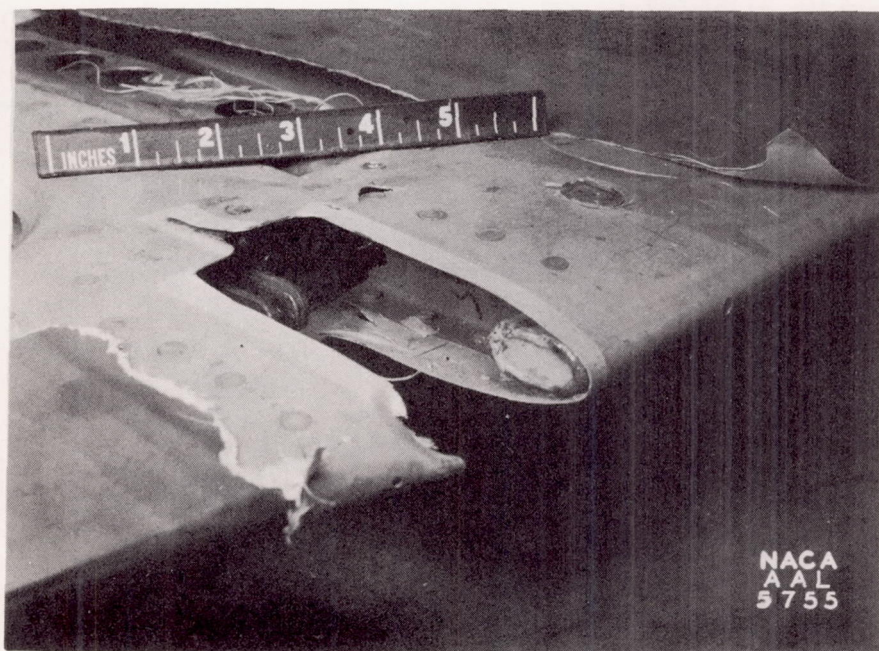


Figure 21.- Lower surface of left elevator showing failure of elevator nose rib at left outboard hinge fitting.

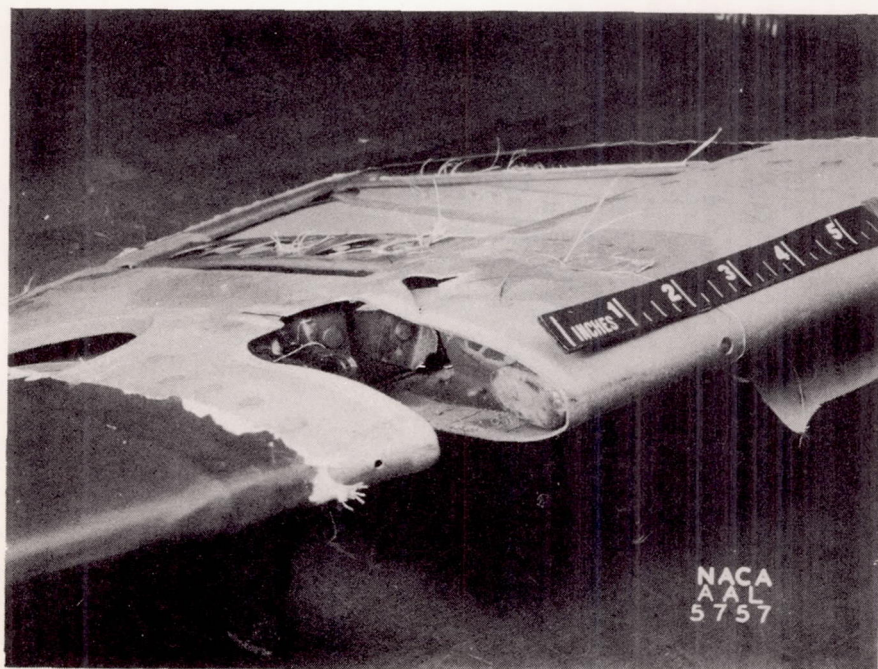


Figure 22.- Upper surface of right elevator showing failure of elevator nose rib at right outboard hinge fitting.

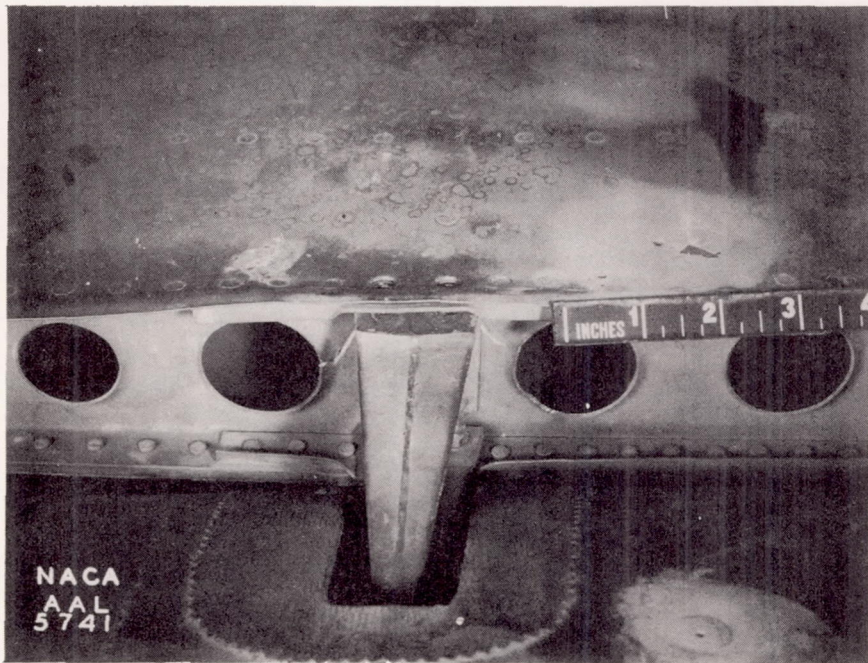


Figure 23.- Detail of cracked stabilizer rear spar at left inboard elevator hinge bracket.

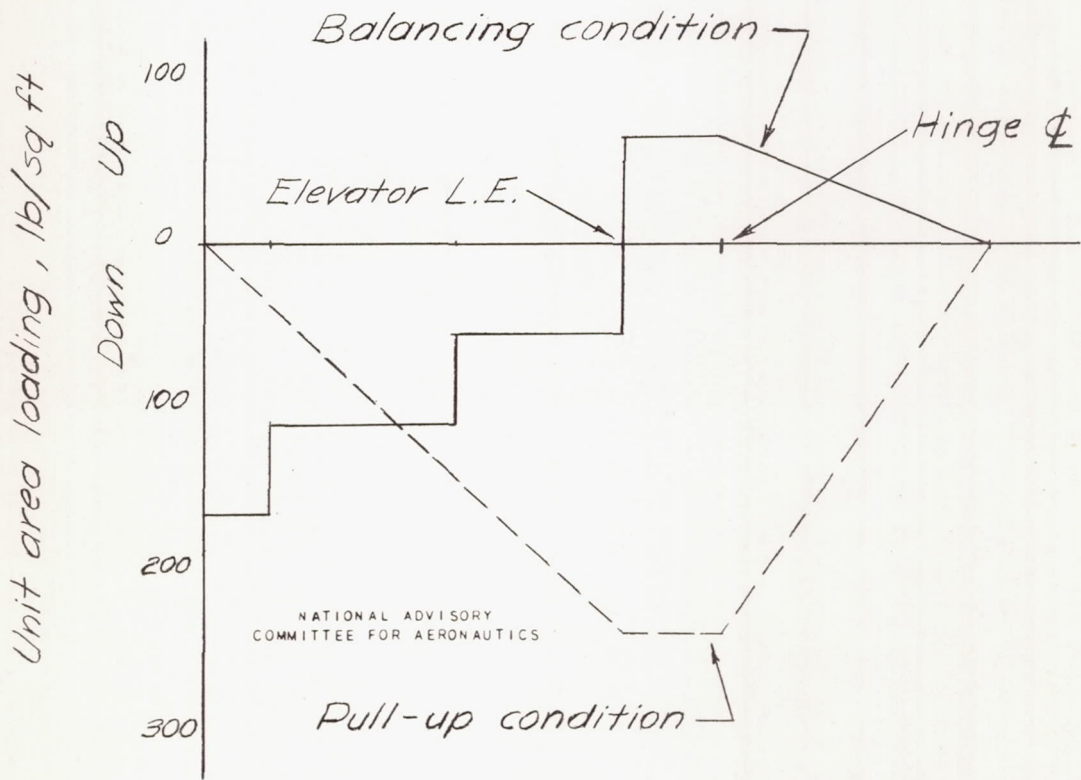


Figure 24 . - Horizontal tail design load conditions.

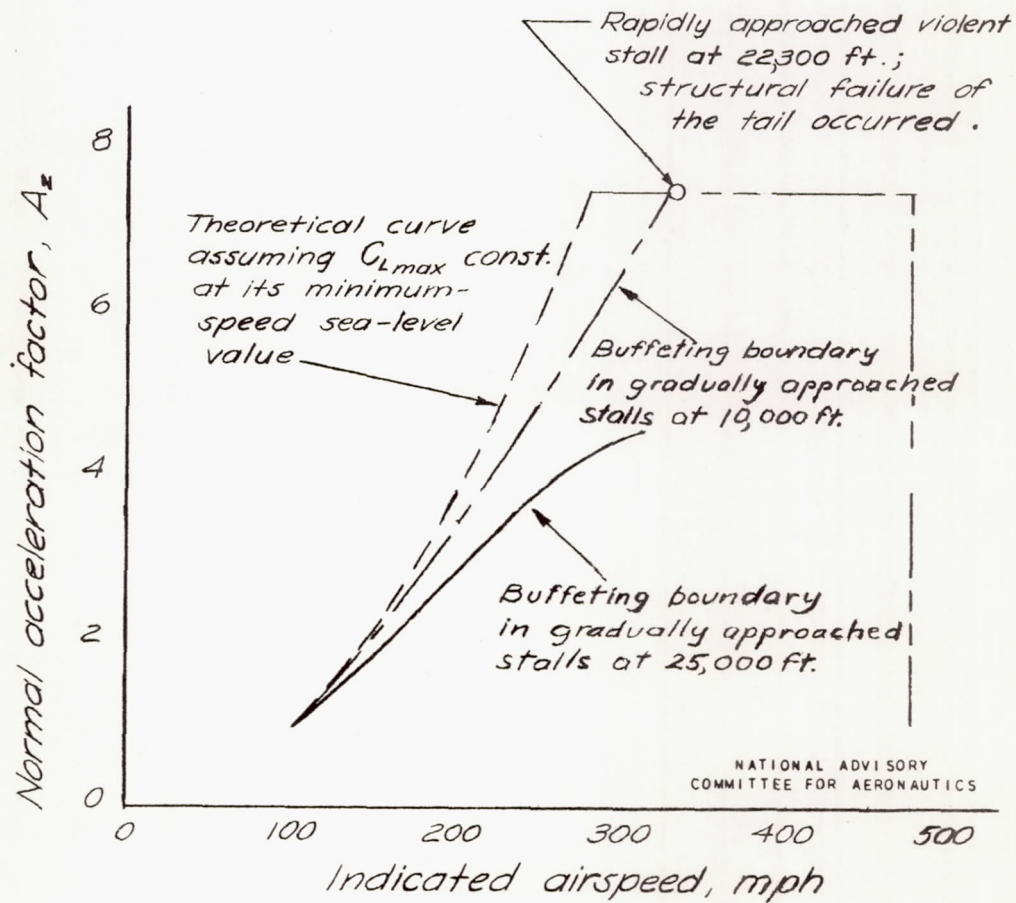


Figure 25. - Positive speed-strength diagram for power-off flight. Test airplane.